

COMPARATIVE MORPHOLOGY AND ULTRASTRUCTURE OF OLFACTORY  
EPITHELIA IN PLETHODONTID SALAMANDERS: EFFECT OF LIFE HISTORY  
VARIATION

By

Emily Gremling

A Thesis Presented to

The Faculty of California State Polytechnic University, Humboldt

In Partial Fulfillment of the Requirements for the Degree

Master of Science in Biology

Committee Membership

Dr. John Reiss, Committee Chair

Dr. Karen Kiemnec-Tyburczy, Committee Member

Dr. Sharyn Marks, Committee Member

Dr. Allison Bronson, Committee Member

Dr. Paul Bourdeau, Program Graduate Coordinator

May 2024

## ABSTRACT

### COMPARATIVE MORPHOLOGY AND ULTRASTRUCTURE OF OLFACTORY EPITHELIA IN PLETHODONTID SALAMANDERS: EFFECT OF LIFE HISTORY VARIATION

Emily Gremling

Many amphibian species rely on olfaction for locating prey and for social interactions during different life stages. Despite the importance of the olfactory system, research on its structure has been taxonomically limited. The most diverse family of salamanders, the Plethodontidae, has been largely excluded from research efforts to describe olfactory morphology. Although several histological studies have been conducted, no studies have yet looked at morphology at the level of ultrastructure using electron microscopy. The primary goal of my research was to examine olfactory morphology and ultrastructure in plethodontid species with a range of life history strategies, to better understand the relationship between habitat, life history, and morphology. Utilizing standard histology, transmission electron microscopy, and MicroCT scanning, I examined four species within Plethodontidae, *Batrachoseps attenuatus*, *Gyrinophilus porphyriticus*, “*Eurycea bislineata*” (a species complex), and *Eurycea troglodytes*, and one outgroup species, *Rhyacotriton variegatus*.

In the direct-developing and biphasic plethodontids I examined, the main olfactory cavity (MOC) of the adult is a sac-like structure with the vomeronasal organ

(VNO) as a lateral diverticulum. The MOC in aquatic stages (larvae and paedomorphic adults) is tubular, extending from the external naris to the choana, with a very small VNO. The ultrastructure in the VNO across all species and stages indicates a stronger correlation between phylogeny and cell type than life history and cell type. In the MOC, I found no apparent correlation between cell types and life stage. I conclude that the cellular composition of the plethodontid MOC may be shaped by both phylogeny and habitat.

## ACKNOWLEDGEMENTS

I would like to express my deepest gratitude to the individuals and institutions that have contributed to the successful completion of this thesis.

First and foremost, I am profoundly thankful to my thesis advisors, Dr. John Reiss and Dr. Karen Kiemnec-Tyburczy, for their support, guidance, and expertise throughout the entire research process. Their invaluable insights and constructive feedback have been instrumental in shaping the direction of this work.

I am also grateful to my undergraduate advisors, Dr. Kenneth Oswald and Dr. Katherine Krynak, whose encouragement and mentorship played a pivotal role in inspiring me to pursue graduate studies. Their belief in my potential made graduate school possible.

I extend my sincere appreciation to the members of my thesis committee, Dr. Sharyn Marks and Dr. Allison Bronson, for their time, valuable feedback, and scholarly input. Their collective wisdom has greatly enriched the quality of this research.

I am grateful to the Department of Biological Sciences at California State Polytechnic University, Humboldt for providing the necessary resources and facilities.

Special thanks Camryn Kenneally, Shea Alexander, Giuseppina (Sun) S. Lanzilli, Ruben Tovar, Mary Kate O'Donnell, and the students in the Highlands Plethodontid course offered in Summer 2022, for assistance in collecting and processing specimens.

I would also like to acknowledge the financial support provided by The National Science Foundation that enabled the execution of experiments and acquisition of essential materials for this project.

Lastly, I extend my deepest gratitude to my family and friends for their encouragement, understanding, and support throughout this academic journey. Their patience and belief in my abilities have been a constant source of motivation.

## TABLE OF CONTENTS

ABSTRACT.....	ii
ACKNOWLEDGEMENTS.....	iv
LIST OF TABLES.....	viii
LIST OF FIGURES.....	ix
LIST OF APPENDICES.....	xi
INTRODUCTION.....	1
METHODS.....	7
Study Species.....	7
Specimen collection.....	9
Standard histology.....	10
Transmission electron microscopy.....	11
Micro-computed tomography (MicroCT).....	12
RESULTS.....	13
Gross morphology.....	13
<i>Rhyacotriton variegatus</i> .....	13
<i>Batrachoseps attenuatus</i> .....	17
<i>Gyrinophilus porphyriticus</i> .....	20
“ <i>Eurycea bislineata</i> ”.....	24
<i>Eurycea troglodytes</i> .....	28
Ultrastructure of cell types.....	31
<i>Rhyacotriton variegatus</i> .....	31

<i>Batrachoseps attenuatus</i> .....	34
<i>Gyrinophilus porphyriticus</i> .....	36
<i>“Eurycea bislineata”</i> .....	41
<i>Eurycea troglodytes</i> .....	44
DISCUSSION .....	47
Gross morphology of the MOC .....	47
Gross morphology of the VNO.....	48
The influence of phylogeny, environment, and life history on olfactory cell types .....	49
REFERENCES .....	60
APPENDICES .....	65

## LIST OF TABLES

Table 1. Summary of species, collection locations, and number used per method .....	9
Table 2. Comparison of previous work on cell types in the amphibian olfactory epithelium with results of the present study. ....	51

## LIST OF FIGURES

Figure 1. Simplified phylogeny of plethodontid salamanders and their relatives .....	8
Figure 2. 3D reconstruction of larval <i>R. variegatus</i> .....	14
Figure 3. Histological sections of larval <i>R. variegatus</i> .....	15
Figure 4. 3D reconstruction of adult <i>R. variegatus</i> .....	16
Figure 5. Histological sections of adult <i>R. variegatus</i> .....	17
Figure 6. 3D reconstruction of adult <i>B. attenuatus</i> .....	19
Figure 7. Histological sections of <i>B. attenuatus</i> .....	20
Figure 8. 3D reconstruction of larval <i>G. porphyriticus</i> .....	21
Figure 9. Histological sections of larval <i>G. porphyriticus</i> .....	22
Figure 10. 3D reconstruction of adult <i>G. porphyriticus</i> .....	23
Figure 11. Histological sections of adult <i>G. porphyriticus</i> .....	24
Figure 12. 3D reconstruction of larval “ <i>E. bislineata</i> ” .....	25
Figure 13. Histological sections of larval “ <i>E. bislineata</i> ” .....	26
Figure 14. 3D reconstruction of adult “ <i>E. bislineata</i> ” .....	27
Figure 15. Histological sections of adult “ <i>E. bislineata</i> ” .....	28
Figure 16. 3D reconstruction of <i>E. troglodytes</i> .....	29
Figure 17. Histological sections of adult <i>E. troglodytes</i> .....	30
Figure 18. Micrographs of the ultrastructure of the MOC in larval <i>R. variegatus</i> .....	31
Figure 19. Micrographs of the ultrastructure of the VNO in larval <i>R. variegatus</i> .....	32
Figure 20. Micrographs of the ultrastructure of the MOC in adult <i>R. variegatus</i> . .....	33
Figure 21. Micrographs of the ultrastructure of the VNO in adult <i>R. variegatus</i> .....	34

Figure 22. Micrographs of the ultrastructure of the MOC in adult <i>B. attenuatus</i> .....	35
Figure 23. Micrographs of the ultrastructure of the VNO in adult <i>B. attenuatus</i> .....	36
Figure 24. Micrographs of the ultrastructure of the MOC in larval <i>G. porphyriticus</i> .....	37
Figure 25. Micrographs of the ultrastructure of the VNO in larval <i>G. porphyriticus</i> .....	38
Figure 26. Micrographs of the ultrastructure of the MOC in adult <i>G. porphyriticus</i> .....	39
Figure 27. Micrographs of the ultrastructure of the VNO in adult <i>G. porphyriticus</i> .....	40
Figure 28. Micrographs of the ultrastructure of the MOC in larval “ <i>E. bislineata</i> ” .....	41
Figure 29. Micrographs of the ultrastructure of the VNO in larval “ <i>E. bislineata</i> ” .....	42
Figure 30. Micrographs of the ultrastructure of the MOC in adult “ <i>E. bislineata</i> ”.....	43
Figure 31. Micrographs of the ultrastructure of the VNO in adult “ <i>E. bislineata</i> ” .....	44
Figure 32. Micrographs of the ultrastructure of the MOC in <i>E. troglodytes</i> . .....	45
Figure 33. Micrographs of the ultrastructure of the VNO in <i>E. troglodytes</i> .....	46
Figure 34. Simplified phylogeny of plethodontid salamanders and their relatives showing cell types present in the MOC .....	54
Figure 35. Simplified phylogeny of plethodontid salamanders and their relatives showing cell types present in the VNO. ....	56

## LIST OF APPENDICES

Appendix A: Specimen Data .....	65
Appendix B: MicroCT Data.....	72

## INTRODUCTION

Olfaction is a sensory modality that enables an organism to detect chemicals in the external environment via the function of specific sensory organs. Because many amphibian species live both in water and on land at different phases of their life cycle (Duellman & Trueb, 1986), the amphibian olfactory system must be able to function for both aquatic and aerial olfaction (Reiss & Eisthen, 2008; Stuelpnagel & Reiss, 2005). Many amphibian species--particularly caudate amphibians (salamanders)--rely on olfaction for locating prey and for social interactions during their different life stages in water and on land (Arnold et al., 2017; Gillette, 2002).

The olfactory system of salamanders is composed of two major parts on each side: the main olfactory cavity (MOC) and the vomeronasal organ (VNO) (Jurgens, 1971; Reiss & Eisthen, 2008). Each MOC has an external, incurrent naris and an internal, excurrent naris (or choana) that opens to the buccal cavity, allowing water or air to flow through it. In larvae, the MOC has a tubular shape extending from the external naris to the choana, and the VNO is a small, ventrolateral projection from the MOC that does not connect to the buccal cavity (Reiss & Eisthen, 2008). In terrestrial, metamorphosed adults, the MOC has a more sac-like structure (Reiss & Eisthen, 2008; Dawley, 2017), and the VNO is a larger lateral diverticulum that connects to the buccal cavity at a region called the lateral palatal groove (Reiss & Eisthen, 2008).

Our knowledge of olfactory organ morphology in salamanders across different life stages and habitats is based on a relatively small number of studies. Traditionally,

most interest has focused on the VNO because the VNO is a synapomorphy for tetrapods; it is present in amphibians and amniotes but is absent in fishes (Eisthen et al., 1994; Parsons, 1967; Silva & Antunes, 2017). Comparative research on salamanders supports the hypothesis that a large VNO correlates with a more terrestrial adult phase, whereas more aquatic species have poorly developed VNOs that are smaller or reduced to a strip of vomeronasal epithelium on the lateral portion of the MOC (Jurgens, 1971).

Functionally, it has been proposed that olfactory detection is partitioned between the two organ systems (Silva & Antunes, 2017). The epithelium of the VNO appears to be primarily used for the detection of nonvolatile odorants such as pheromones, in both aquatic and terrestrial environments (Baxi et al., 2006; but see also Silva & Antunes, 2017). The MOC of caudates (and other tetrapods), on the other hand, is thought to detect water-borne odorants in the aquatic environment but volatile odorants in the terrestrial environment, though this characterization is not very well supported (Baxi et al., 2006).

The sensory function of an olfactory organ necessarily depends on the cells that comprise that organ. At the tissue level, the MOC and VNO are lined with regions of sensory (olfactory) and nonsensory epithelium. A detailed study that compared paedomorphic adults, terrestrial adults, and aquatic larvae of the salamander *Dicamptodon tenebrosus* (Family Dicamptodontidae) found that in aquatic larvae and paedomorphic adults of *D. tenebrosus* the MOC contains ridges of non-sensory epithelium that separate valleys lined with sensory epithelia (Stuelpnagel & Reiss, 2005). During metamorphosis, the MOC and VNO are dorsoventrally flattened, the ridges in the MOC are reduced and the VNO becomes better developed (Stuelpnagel & Reiss, 2005).

Specialization for aquatic vs. terrestrial olfaction is also apparent at the cellular level in *D. tenebrosus*. The olfactory epithelium of all vertebrates contains three cell types: basal (stem) cells, olfactory sensory receptor cells, and supporting cells (Dawley, 2017). Aquatic stages (larvae and paedomorphs) of *D. tenebrosus* (Stuelpnagel & Reiss, 2005) have four cell types in the MOC: ciliated and microvillar receptor cells, and ciliated and secretory supporting cells. These cell types are also present in terrestrial adults, but the presence of all four cell types is restricted to the lateral floor of the MOC, while the medial floor and roof of the MOC (= “predominant olfactory epithelium”) have only three: they lack ciliated supporting cells. By analogy with the organization observed in frogs (Benzekri & Reiss, 2012), the lateral MOC is likely being used for aquatic (“water-smelling”) olfaction, while using the medial MOC for terrestrial (“air-smelling”) olfaction. (In frogs, however, the “air-smelling” epithelium of the MOC has only ciliated receptor cells and secretory supporting cells; it lacks microvillar receptor cells.)

The VNO in all stages of *D. tenebrosus* contains an epithelium of microvillar receptor cells and secretory and ciliated supporting cells, suggesting that its function does not change during metamorphosis (Stuelpnagel & Reiss, 2005). Across other salamanders, however, there is much variation in the distribution of receptor and supporting cell types of the MOC and VNO, and this is not obviously correlated with aquatic vs. terrestrial olfaction, or with phylogeny (reviewed by Benzekri & Reiss, 2012; see also discussion, below).

Given the current paucity of data on cell types of the salamander olfactory system and especially their relation to aquatic vs. terrestrial olfaction, a comparative study of

olfactory morphology and ultrastructure across a phylogenetically restricted group with species that have both aquatic and terrestrial life history phases may provide some insight into the significance of variation seen. The salamander family Plethodontidae provides an excellent opportunity for such a study. The family includes approximately two-thirds of living caudate species and exhibits such diversity due to the adaptive radiation they have undergone; adults can be found in many distinct habitats throughout North America, South America, Europe, and Asia (Pyron & Wiens, 2011; Wake, 1966). There are several traits that all plethodontids share, including lunglessness and the presence of nasolabial grooves (Wake, 1966).

Life history strategies within Plethodontidae range from direct development, in which there is no larval stage, to a biphasic life cycle with an aquatic larval stage followed by metamorphosis into a more terrestrial adult, to paedomorphosis, in which larval features are retained by the adult (Beachy et al., 2017). While there is some debate about which life history strategy is ancestral for this group (Beachy et al., 2017; Bonett et al., 2014a), the biphasic life history is most strongly supported as being the most ancestral state, with both direct development (e.g., *Batrachoseps attenuatus*) and paedomorphosis (e.g., *Eurycea troglodytes*, *E. wallacei*) evolving several times independently. This diversity thus provides a chance to investigate correlations between life history and phenotype in a monophyletic group.

Terrestrial plethodontid salamanders rely on olfaction (including vomerolfaction) for a variety of social behaviors, including courtship, territory recognition, and prey detection (Brown, 1968; Gillette, 2002). For example, during the approach phase of

courtship, male plethodontids (and males in the closely related family Rhyacotritonidae) gather olfactory cues left by females by nose-tapping on a substrate (Arnold et al., 2017). And *Batrachoseps attenuatus* uses nose-tapping behavior to differentiate between its territory and the territory of conspecifics (Gillette, 2002). Nose-tapping is a terrestrial plethodontid behavior that transports odorants via the nasolabial grooves to the external naris, then into the main olfactory cavity and vomeronasal organ (Brown, 1968). In *Plethodon cinereus*, cauterizing the nasolabial grooves to impair vomeronasal function reduced effectiveness of prey detection and foraging (Placyk & Graves, 2002).

Despite its important function in this vertebrate group, research on the structure of the olfactory system in plethodontids has been limited almost exclusively to histological studies on adults (e.g., Dawley, 2017; Dawley & Bass, 1988). These results suggest that the gross morphology of the plethodontid olfactory organ may remain consistent despite differences in developmental mode. For example, although they have evolved different life history strategies, the pattern of adult *Eurycea* nasal morphology is very similar to that of *Plethodon*, a direct-developing genus, as well as adults of a variety of other plethodontid genera (Dawley, 2017). For biphasic species, the only histology to date that includes larvae are the early studies on *Eurycea bislineata* by Wilder (1925). Wilder (1925) showed that the VNO begins developing during the late stages of the larval period and does not fully develop until post-metamorphosis, indicating that the VNO plays a larger role in aerial olfaction than aquatic olfaction.

In sum, despite the research done to understand the structural and correlates of olfaction in water compared to that in air, we still lack the data needed to make rigorous

comparisons of olfactory anatomy among closely related species with varying life histories. We also know nothing about the specific cell types present in the olfactory epithelium of plethodontids, because no previous studies have looked at morphology at the level of ultrastructure using electron microscopy. Thus, the goal of my project was to examine plethodontid olfactory morphology in four species with a variety of life history modes, and in one outgroup species, using standard histology and electron microscopy.

The specific hypotheses I wanted to evaluate were:

1. Patterns of olfactory organization are consistent across species with the same life history strategy, regardless of evolutionary history.
2. Patterns of olfactory organization in paedomorphic species are consistent with the larvae of closely related species.
3. Aquatic olfactory features are lost (or reduced) in terrestrial, direct-developing species.

## METHODS

### Study Species

To research the impacts of life history variation on olfactory morphology, I examined four species within the plethodontid subfamily Hemidactyliinae, and one species, *Rhyacotriton variegatus*, belonging to a different caudate family (Rhyacotritonidae) (Fig. 1). I selected species within Hemidactyliinae in order to sample the variety of life history strategies present in this subfamily. Within *Eurycea*, I examined larvae and metamorphosed adults from the biphasic species *E. bislineata* and *E. wilderae* in the *E. bislineata* species complex (Kozak et al., 2005), which I will refer to together as “*E. bislineata*” for brevity. I also examined paedomorphic representatives of *E. troglodytes*, a species that has some paedomorphic populations and some that have re-evolved a biphasic life history (Bonett et al., 2014). I examined larvae and adults of *Gyrinophilus porphyriticus*, a species that has a biphasic life history (Bruce, 1978). *Gyrinophilus* is the sister group to *Eurycea* (Pyron & Wiens, 2011; Shen et al., 2016). I also examined *Batrachoseps attenuatus*, which has direct development. Within Rhyacotritonidae, I examined larvae and adults of *R. variegatus*, a biphasic species.

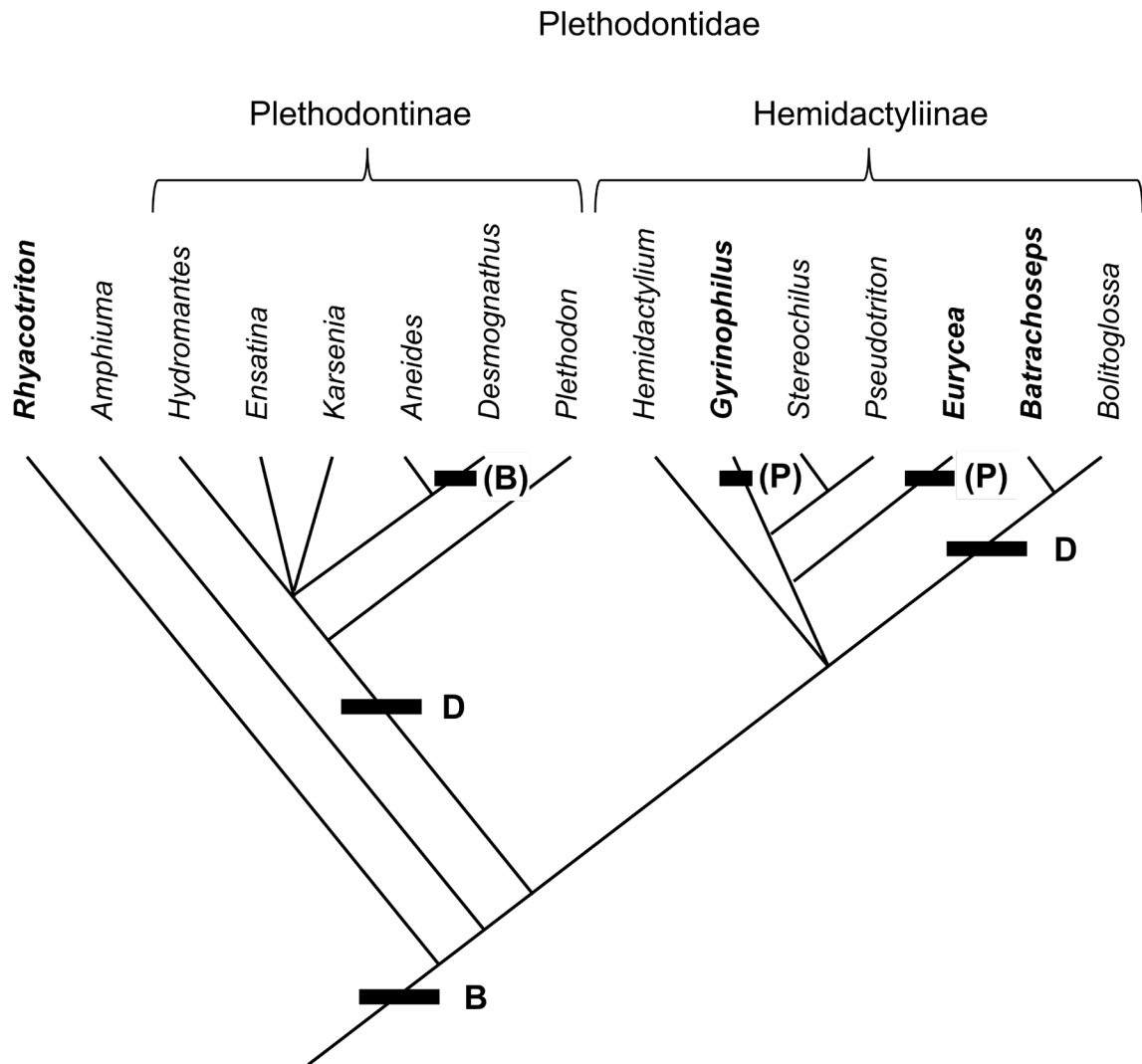


**Figure 1.** Simplified phylogeny of plethodontid salamanders and their relatives with life history strategies: biphasic (B), paedomorphic (P), and direct developing (D). Parentheses indicate life history strategies that are present in some but not all members of the genus. (Consensus tree based on Pyron and Wiens [2011] and Shen et al. [2016]). Genera in bold are those examined in this study.

## Specimen collection

Specimens were collected by hand and dip net in accordance with Cal Poly Humboldt IACUC protocol (2020B93-A). Collecting permits were obtained from California (Collecting Permit S-200260005-20362-001) and Virginia (Collecting Permit 071078); no permit was required for North Carolina specimens because I had fewer than 25 animals per collector. *Eurycea troglodytes* specimens were graciously donated by Ruben Tovar, and some *Gyrinophilus porphyriticus* specimens were contributed by Mary Kate O'Donnell. A summary of all specimens used and their disposition is given in Table 1 (see Appendix A for detailed information on each specimen).

*Table 1. Summary of species, collection locations, and number used per method (histology, TEM, or MicroCT scanning)*

<b>Species</b>	<b>Collection Location</b>	<b>Standard Histology (n)</b>	<b>TEM (n)</b>	<b>MicroCT Scanning (n)</b>
<i>Rhyacotriton variegatus</i> larvae	Humboldt County, CA	3	3	1
<i>R. variegatus</i> adults	Humboldt County, CA	5	2	1
<i>Batrachoseps attenuatus</i> adults	Humboldt County, CA	3	8	2
<i>Gyrinophilus porphyriticus</i> larvae	Jackson County, NC Rockingham County, VA	3	5	1
<i>G. porphyriticus</i> adults	Jackson County, NC Rockingham County, VA Lycoming County, PA	2	4	1
“ <i>Eurycea bislineata</i> ” larvae	Jackson County, NC Rockingham County, VA	7	5	1
“ <i>E. bislineata</i> ” adults	Jackson County, NC Rockingham County, VA	4	6	1
<i>E. troglodytes</i> adults	Kerr County, TX	6	4	1

### Standard histology

Specimens were euthanized immediately after collection by overdose with 0.1 M MS222 (tricaine methane sulfonate, Western Chemical) buffered with sodium bicarbonate to pH 7.0. Before fixation, I measured snout-vent length (SVL) and total length (TL) and dissected the abdomen to view reproductive organs and determine sex. I then removed the heads of the specimens and fixed them in 10% neutral buffered formalin. Heads were processed for histology by decalcification in RDO (Apex Engineering, Aurora, IL), dehydration through a graded series of ethyl alcohol concentrations, clearing in toluene, and embedding in Paraplast®. A rotary microtome was used to section the embedded specimen at 10 µm. These sections were fixed onto slides using Haupt's Solution and a 3% formalin solution, and after dewaxing, the slides were stained with Delafield's hematoxylin and eosin (Humason, 1979).

Standard histology was used to visualize the shape and orientation of the MOC and VNO as well as classify tissue within these cavities as sensory (olfactory) or nonsensory. The classification was based on the description of previous histological studies on plethodontid salamanders (e.g., Dawley, 2017; Dawley & Bass, 1988). Sensory tissue (epithelium) was identified by being thicker compared to nonsensory tissue, and having basal nuclei that stain very dark. In contrast, nonsensory tissue was typically thinner compared to sensory tissue and had more superficial nuclei.

## Transmission electron microscopy

I used transmission electron microscopy (TEM) to describe the cell types present in the MOC and VNO. For each species, I collected data on a minimum of three individuals per species or three individuals per stage for biphasic species. The snouts of specimens were fixed in 2.5% glutaraldehyde in 0.05M cacodylate buffer (pH=7.2), postfixed in 1.5% osmium tetroxide, embedded in Spurr's resin (Bazzola & Russell, 1992), sectioned using a Reichert Om U2 ultramicrotome, stained with lead citrate and uranyl acetate, and examined on a Hitachi 7800, Philips Tecnai 12, or Philips EM 208S transmission electron microscope.

Cells of sensory epithelia were characterized as one of four cell types: ciliated receptor cells, microvillar receptor cells, ciliated supporting cells, or secretory supporting cells. Characteristics used to determine cell type were based on previous studies on the ultrastructure of olfactory morphology in amphibians (e.g., Hansen et al., 1998; Stuelpnagel & Reiss, 2005). I used the presence of an olfactory knob to identify receptor cells, which would then be further classified by the presence of cilia or microvilli. I used the presence of a terminal web or a broader cell (the lack of an olfactory knob) to identify supporting cells, which would be further classified by the presence of secretory vesicles or cilia.

### Micro-computed tomography (MicroCT)

One individual from each life stage per species was processed for MicroCT scanning and 3-D reconstruction of the nasal cavity. Specimens were fixed in 10% neutral-buffered formalin, rinsed with water, and stained with 1% Lugol's iodine (Humason, 1979) for two days. Specimens were scanned using a Nikon XTH-225 MicroCT scanner and the resulting image stacks were processed using FIJI (Schindelin et al., 2012) and 3D Slicer ([slicer.org](http://slicer.org)) for segmentation of olfactory structures and their 3D reconstruction. See Appendix B for supplemental data on MicroCT scanning parameters.

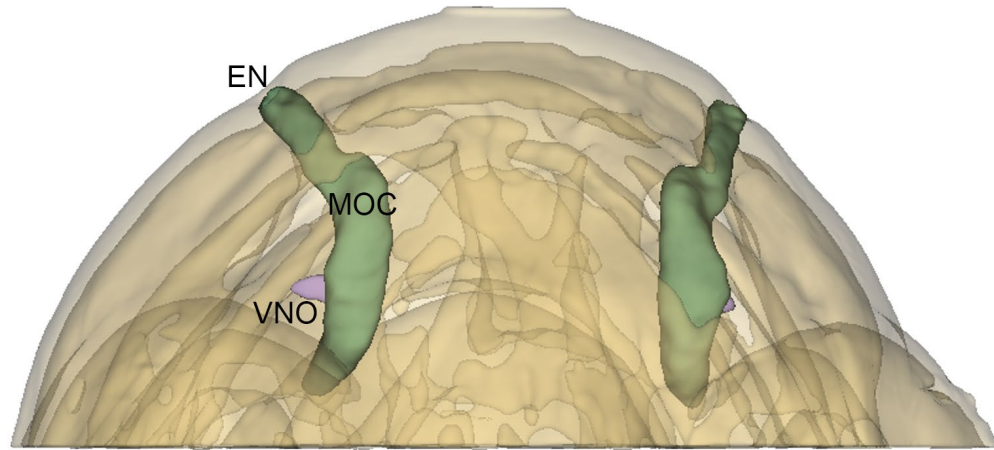
## RESULTS

### Gross morphology

#### *Rhyacotriton variegatus*

The MOC of larval *R. variegatus* is a slender tube that begins at the external naris and extends posteriorly until it ends at the choana (Figs. 2 and 3A). In the larval stage, the VNO is a relatively small lateral projection (Figs. 2 and 3D). The sensory tissue (ST) in the anterior portion of the MOC is concentrated along the medial wall (Fig. 3C), however as the MOC extends posteriorly the sensory tissue is distributed throughout the MOC (Fig. 3D) and extends beyond the choana (Fig. 3E). However, the sensory tissue is not distributed throughout the cavity more posteriorly (Fig. 3E); there is nonsensory tissue (NT) present along the floor and lateral wall of the MOC near the choana.

A.



B.

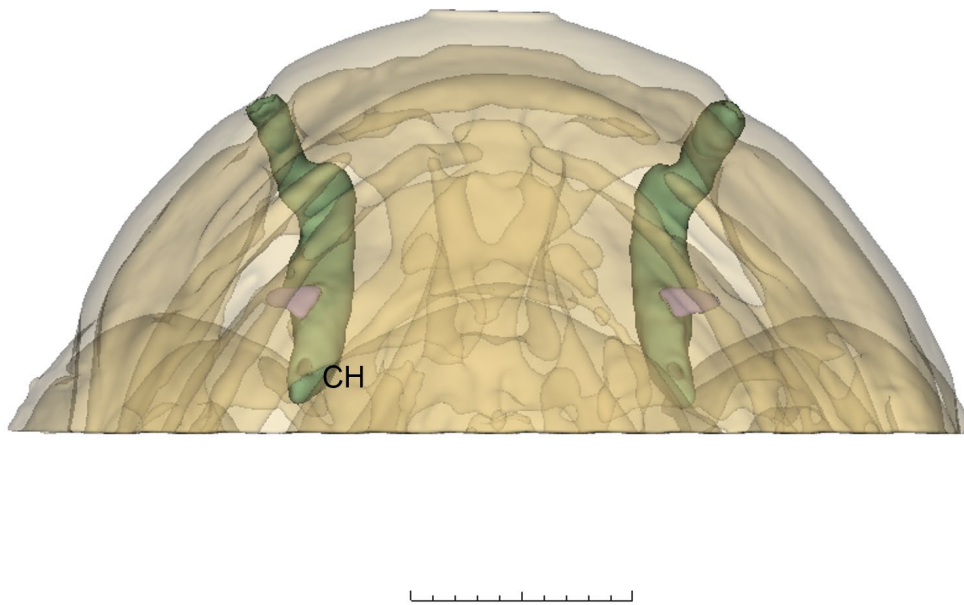


**Figure 2.** 3D reconstruction of larval *R. variegatus* showing the MOC (green), VNO (purple), external naris (EN) and choana (CH). Dorsal view (A) and ventral view (B). Scale bar = 0.09 cm.

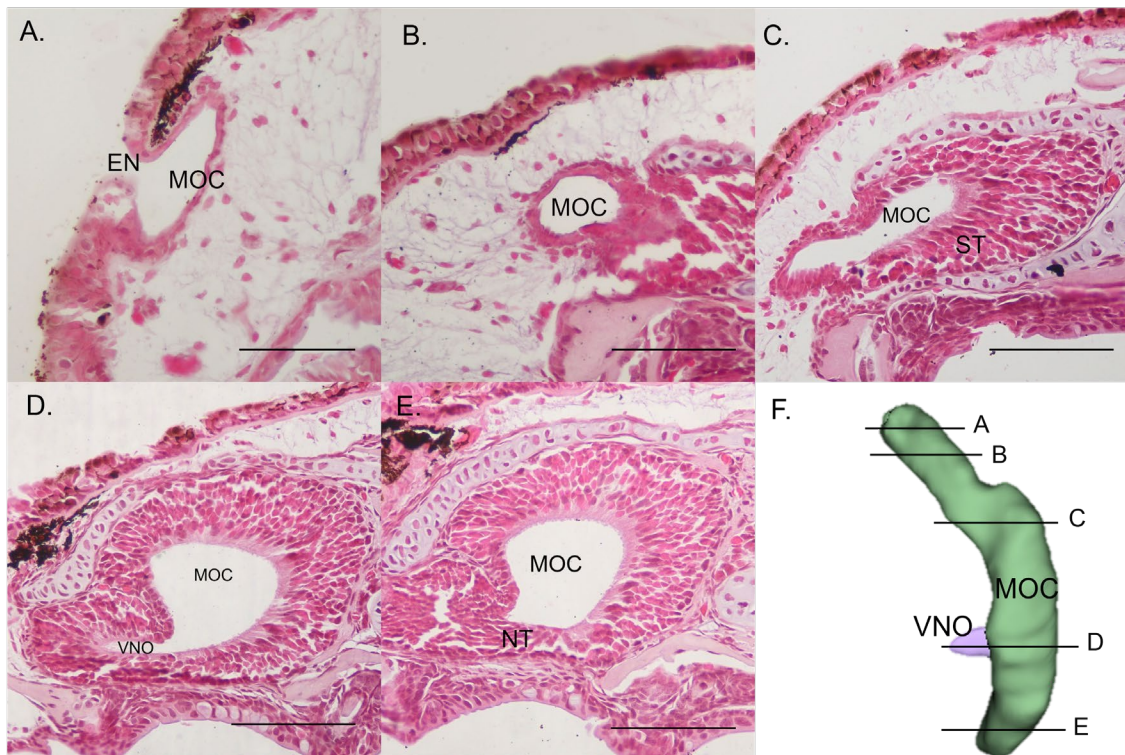
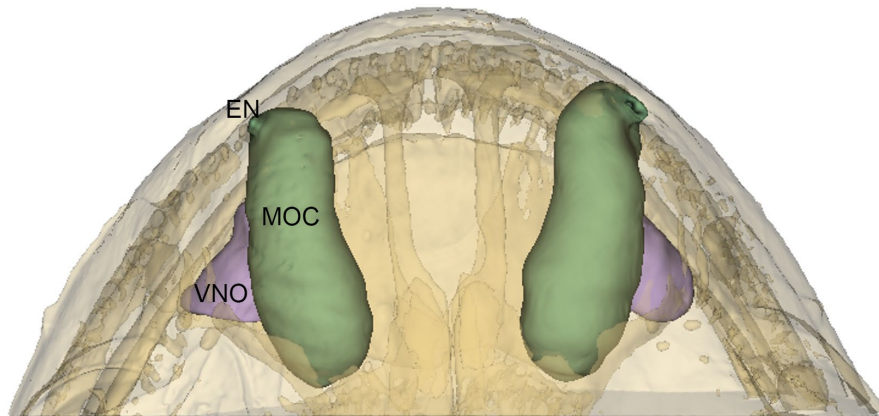


**Figure 3.** *A-E*) Histological sections of larval *R. variegatus* taken transversely through the nasal cavity from anterior to posterior, showing the external naris (EN), main olfactory cavity (MOC), vomeronasal organ (VNO), choana (CH) sensory tissue (ST) and nonsensory tissue (NT). *F*) 3D reconstruction with approximate section locations. Scale bar = 0.2 mm

After metamorphosis, significant changes have occurred. The MOC of adult *R. variegatus* is a sac-like structure that begins just anterior to the external naris (Figs. 4 and 5). The MOC extends posteriorly until it ends at the choana. In the adult stage the VNO is relatively larger and more developed (Figs. 4 and 5). The sensory tissue is thick and distributed around the MOC and VNO at the anterior ends of these cavities (Fig. 5A-D) but gradually thins and is replaced by nonsensory tissue more posteriorly. At the choana, the epithelium is mostly nonsensory epithelium that lines the MOC and lateral palatal groove (LPG) with some sensory tissue still present along the roof of the MOC (Fig 5E).

A.



B.

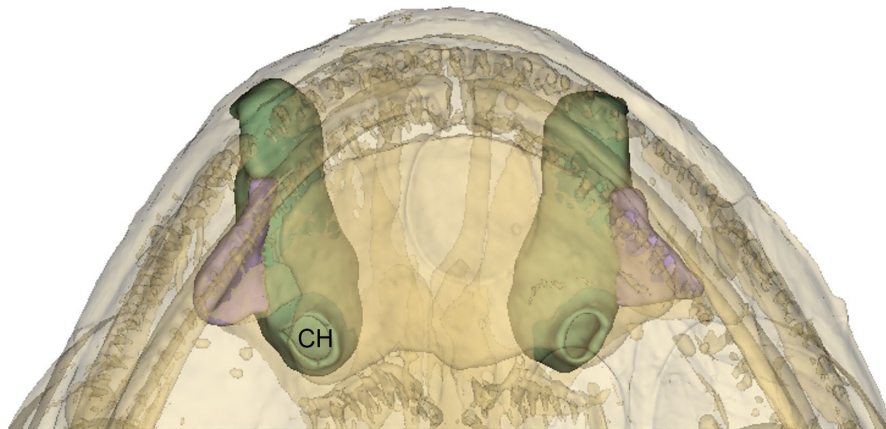


**Figure 4.** 3D reconstruction of adult *R. variegatus* showing the MOC (green), VNO (purple) external naris (E), and choana (CH). Dorsal view (A) and ventral view (B). Scale bar = 0.23 cm.

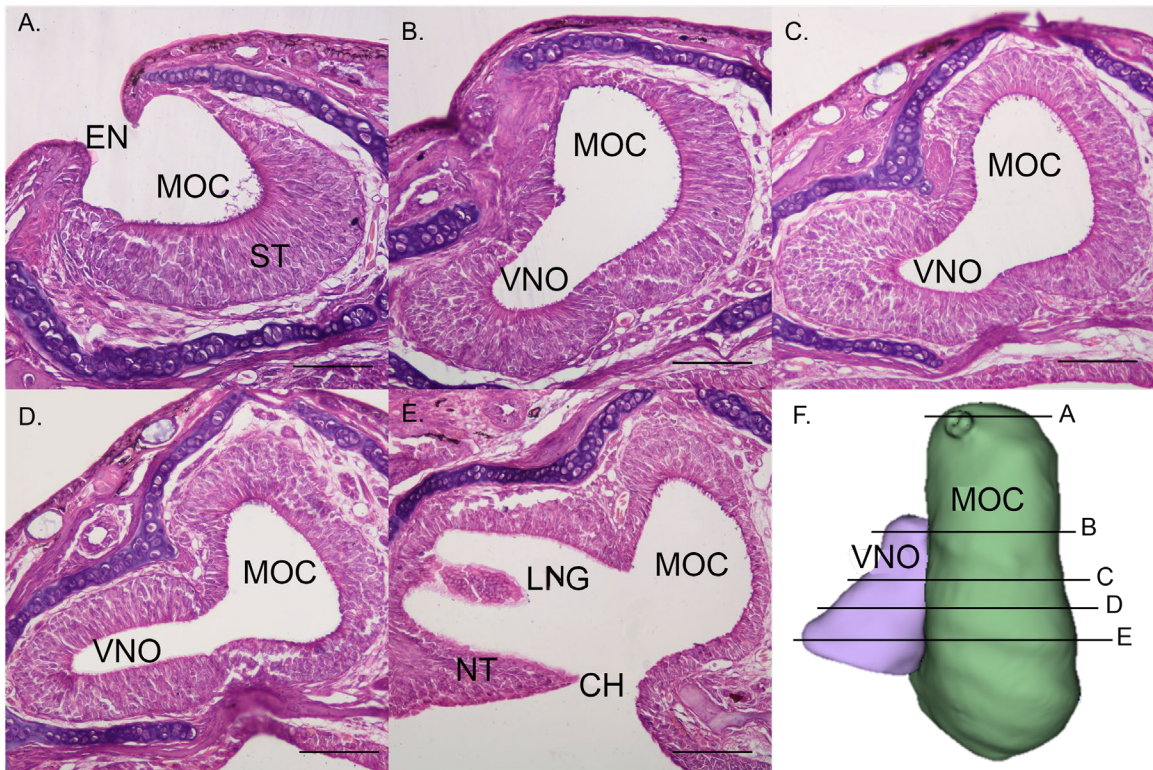


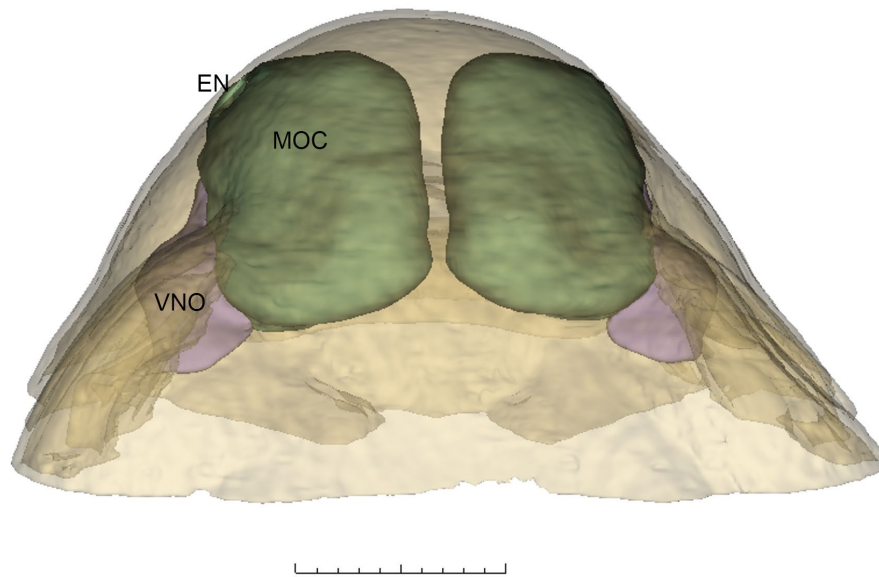
**Figure 5.** *A-E*) Histological sections of adult *R. variegatus* taken transversely through the nasal cavity from anterior to posterior, showing the external naris (EN), main olfactory cavity (MOC), vomeronasal organ (VNO), lateral nasal groove (LNG), choana (CH) sensory tissue (ST), and nonsensory tissue (NT). *F*) 3D reconstruction with approximate section locations. Scale bar = 0.2 mm.

*Batrachoseps attenuatus*

The overall shape of the MOC and VNO for *B. attenuatus* is dorsoventrally flattened compared to other species (Figs. 6 and 7). Sensory tissue is present at the anterior portion of the MOC where the external naris first enters the cavity (Fig. 7A). When the sensory tissue is first present it is concentrated along the floor and medial wall of the MOC. As the MOC extends posteriorly the sensory epithelium lines the walls of the MOC and VNO (Fig. 7B and 7C). More posteriorly in the MOC and VNO the

sensory tissue thins out and is replaced with nonsensory tissue, which persists through the choana (Fig. 7D and 7E).

A.



B.

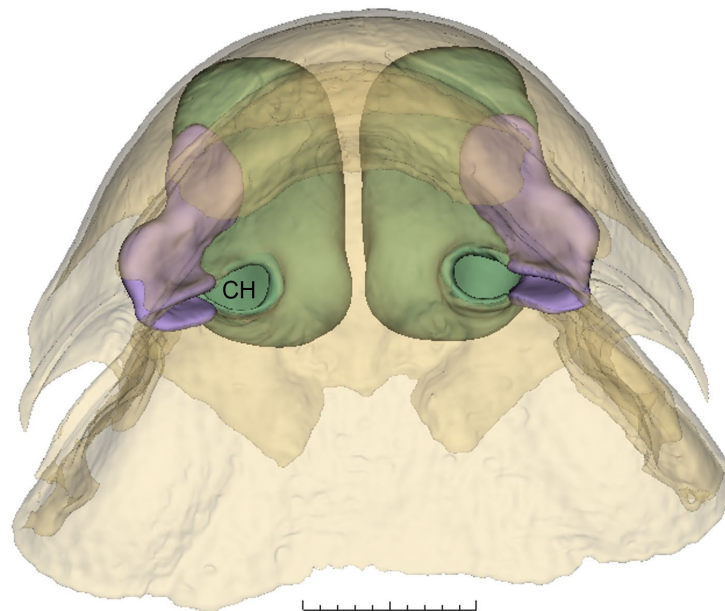


**Figure 6.** 3D reconstruction of adult *B. attenuatus* showing the MOC (green), VNO (purple), external naris (EN), and choana (CH). Dorsal view (A) and ventral view (B). Scale bar = 0.08 cm.

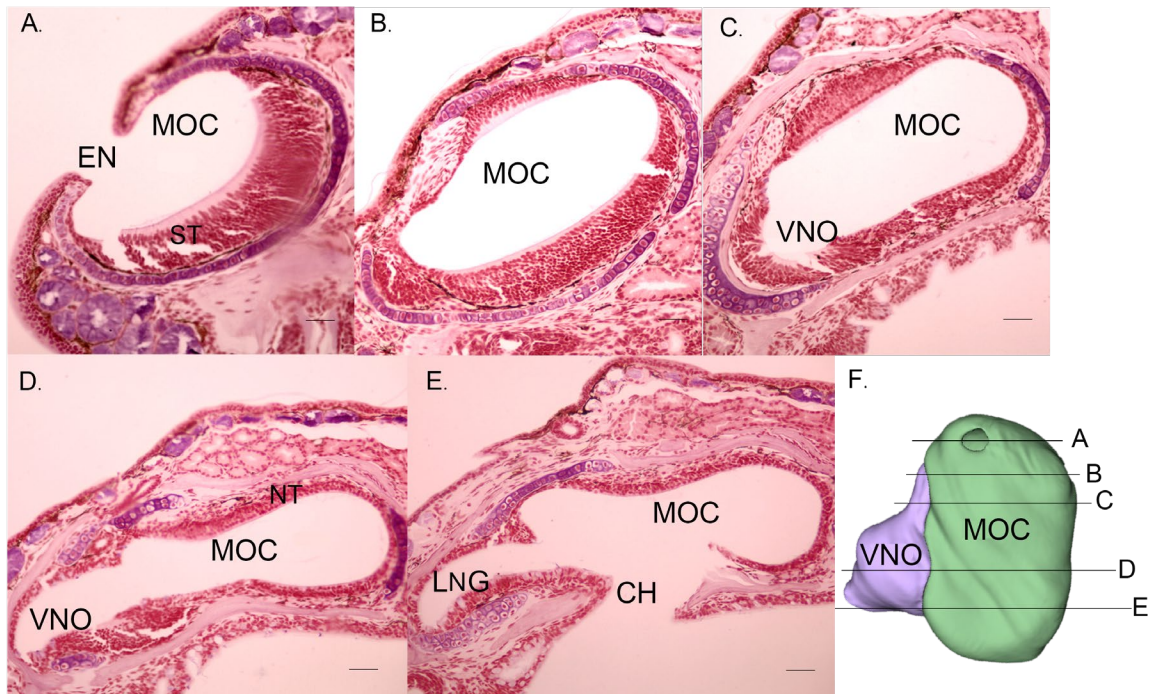
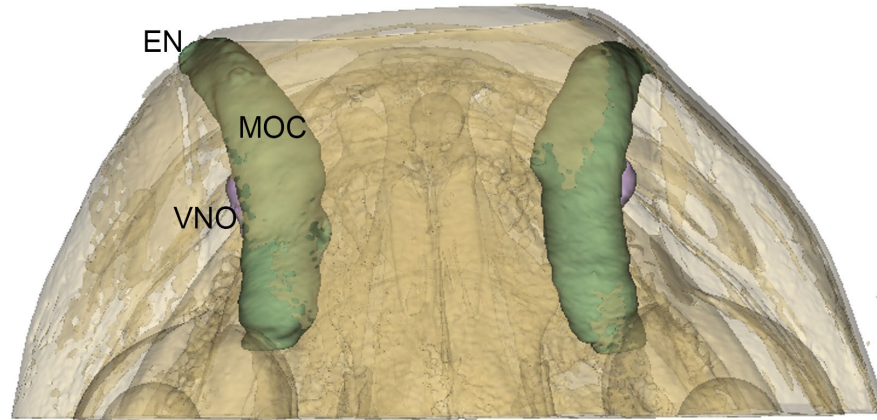


**Figure 7. A-E)** Histological sections of *B. attenuatus* taken transversely through the nasal cavity from anterior to posterior, showing the external naris (EN), main olfactory cavity (MOC), vomeronasal organ (VNO), lateral nasal groove (LNG), choana (CH), sensory tissue (ST), and nonsensory tissue (NT). **F)** 3D reconstruction with approximate section locations. Scale bar = 0.25 mm.

### *Gyrinophilus porphyriticus*

The shape of the MOC and VNO in larval *G. porphyriticus* is similar to that seen in larvae of other species examined in this study. The MOC is slender and elongated with no sensory tissue anterior to the external naris (Figs. 8 and 9). At the anterior end of the MOC the sensory tissue is mostly distributed along the medial wall (Fig. 9B). As the MOC extends posteriorly the sensory tissue is distributed along the entire MOC (Fig. 9C and 9D). At the posterior end near the choana, the sensory tissue is confined to the roof of the MOC while the walls are lined with nonsensory tissue (Fig. 9E). The VNO in the larval stage is smaller than that of the adult stage and is only present as a small lateral projection (Figs. 8 and 9).

A.



B.

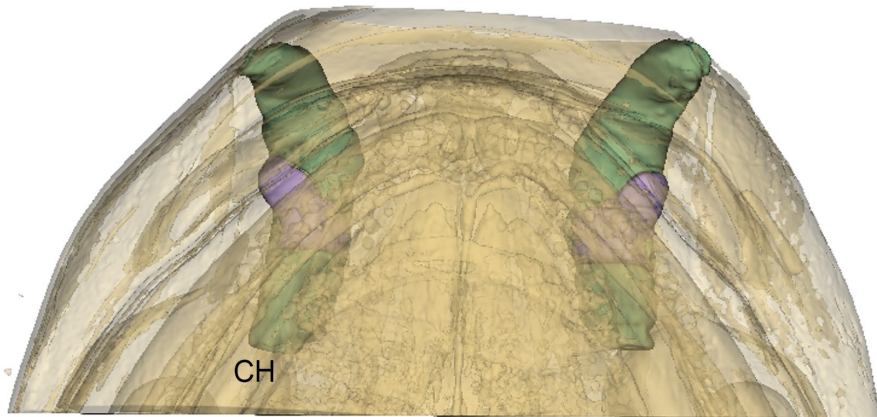


**Figure 8.** 3D reconstruction of larval *G. porphyriticus* showing the MOC (green), VNO (purple) external naris (EN), and choana (CH). Dorsal (A) and ventral (B) view. Scale bar = 0.32 cm.

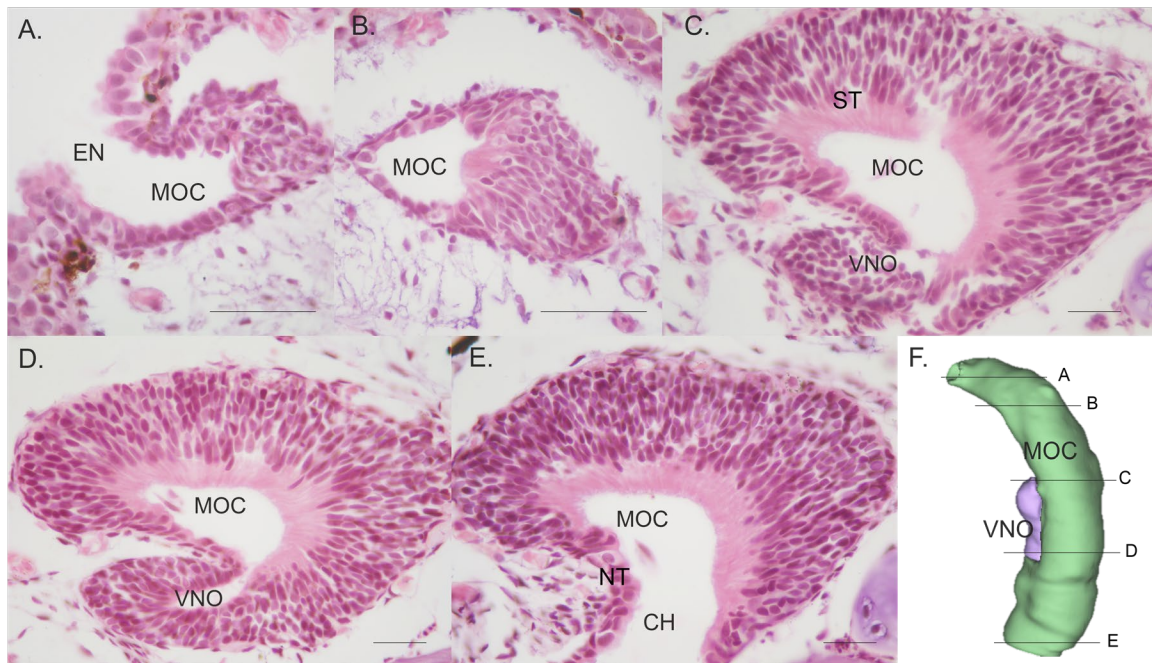


**Figure 9. A-E)** Histological sections of larval *G. porphyriticus* taken transversely through the nasal cavity from anterior to posterior, showing the external naris (EN), main olfactory cavity (MOC), vomeronasal organ (VNO), choana (CH), sensory tissue (ST) and nonsensory tissue (NT). **F)** 3D reconstruction with approximate section locations. Scale bar = 0.5 mm.

The MOC of the adult *G. porphyriticus* begins anterior to the external naris (Figs. 10 and 11). At the external naris, there is a thick sensory tissue on the floor of the MOC (Fig. 11A). As the MOC extends posteriorly, the sensory tissue extends to cover the entire inner wall of the MOC (Figs. 11b and 11C). The VNO extends laterally from the MOC at the anterior end and then again more posteriorly, causing two distinct bulges in the MOC at the anterior end and then again more posteriorly, causing two distinct bulges in the VNO (Fig. 10). The sensory tissue persists in both the MOC and VNO anterior to the choana where it has largely thinned out and been replaced by a nonsensory tissue, making the VNO the lateral nasal groove, which is nonsensory (Figs. 11D and 11E).

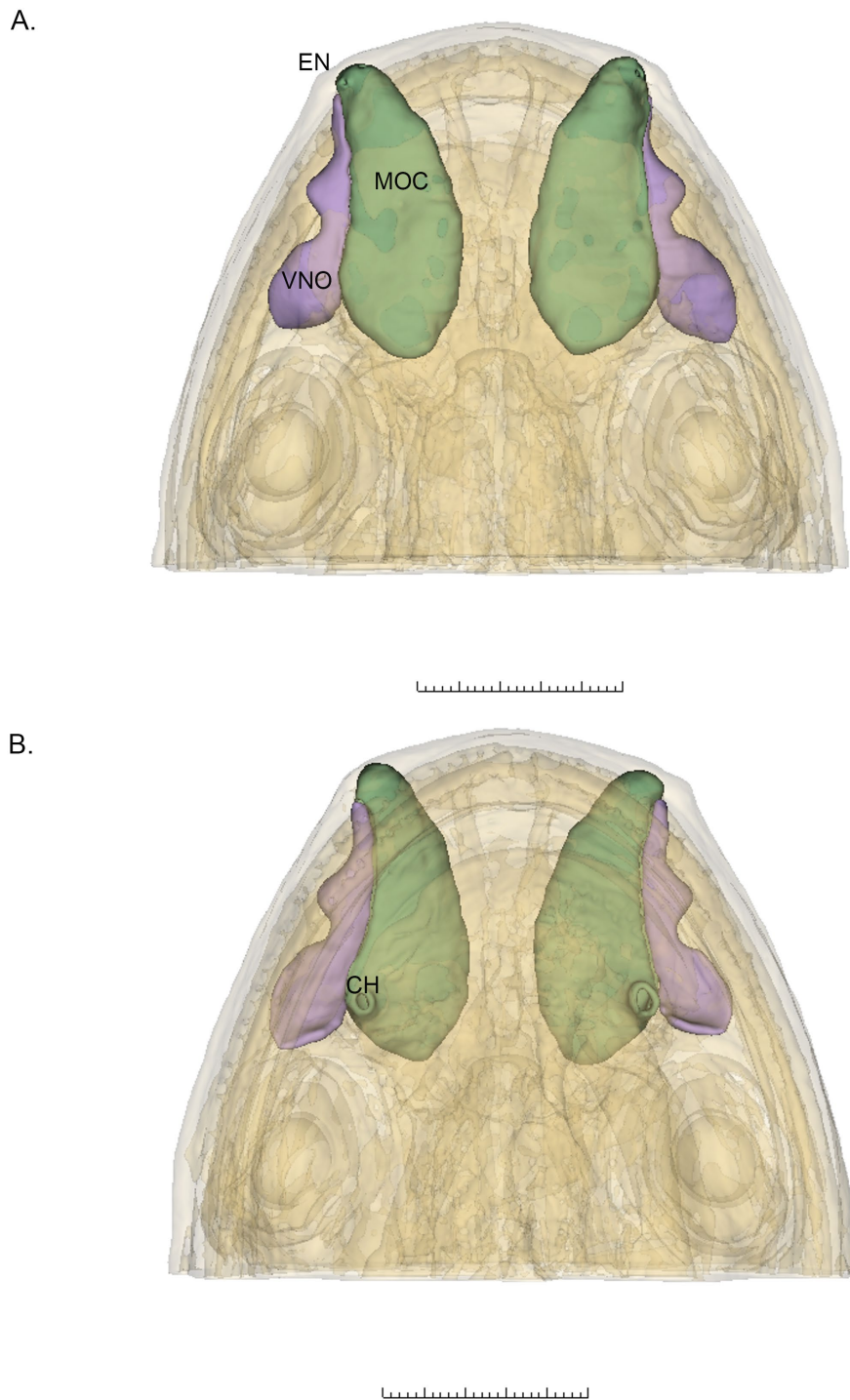


**Figure 10.** 3D reconstruction of adult *G. porphyriticus* showing the MOC (green), VNO (purple), external naris (EN), and choana (CH). Dorsal (A) and ventral (B) view. Scale bar = 0.49 cm.

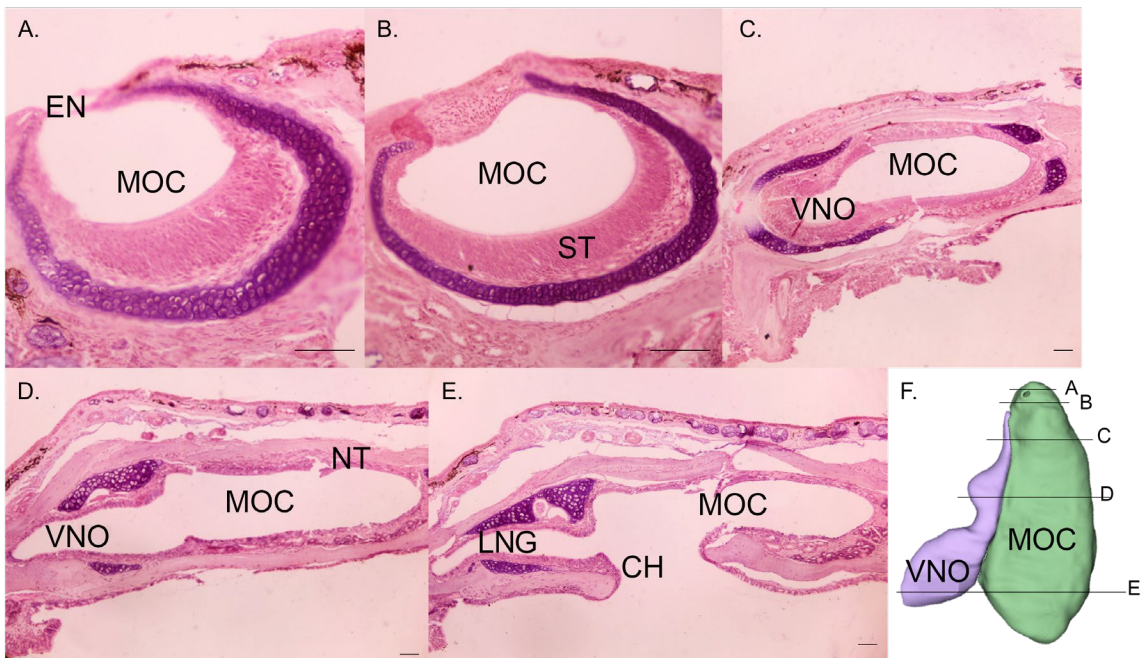
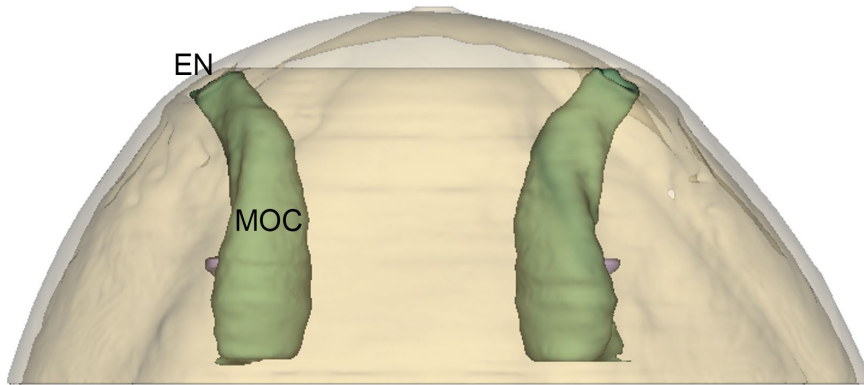


**Figure 11. A-E)** Histological sections of adult *G. porphyriticus* taken transversely through the nasal cavity from anterior to posterior, showing the external naris (EN), main olfactory cavity (MOC), vomeronasal organ (VNO), lateral nasal groove (LNG), choana (CH), sensory tissue (ST) and nonsensory tissue (NT). **F)** 3D reconstruction with approximate section locations. Scale bar = 0.5 mm.

“*Eurycea bislineata*”

The MOC of larval “*E. bislineata*” is a tube-like structure that begins at the external naris and extends posteriorly until it ends at the choana (Figs. 12 and 13). At the anterior end of the MOC, sensory tissue is confined to the medial wall (Fig. 13A). As the MOC extends posteriorly, sensory tissue is present along the entire cavity (Figs. 13C and 13D), although it is thickest along the medial wall. The VNO is a relatively small lateral projection and is also lined with thick sensory tissue (Figs. 12 and 13D). When the MOC ends at the choana, sensory tissue is still present along the roof of the cavity but is replaced with nonsensory tissue on the walls (Fig. 13E).

A.



B.

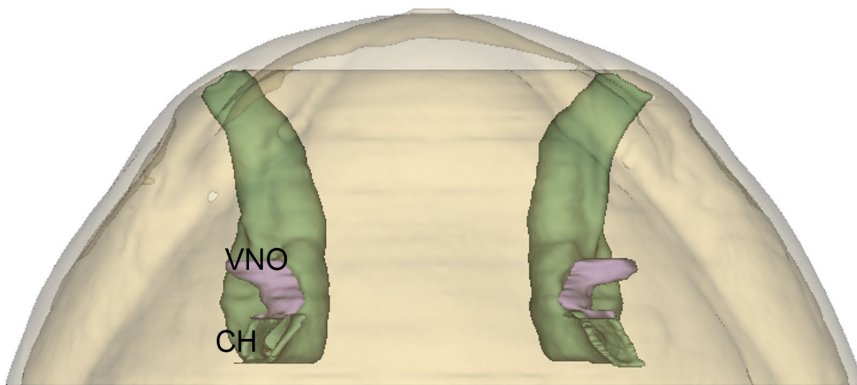


**Figure 12.** 3D reconstruction of larval “*E. bislineata*” showing the MOC (green), VNO (purple) external naris (EN), and choana (CH). Dorsal (A) and ventral (B) view. Scale bar = 0.11 cm.

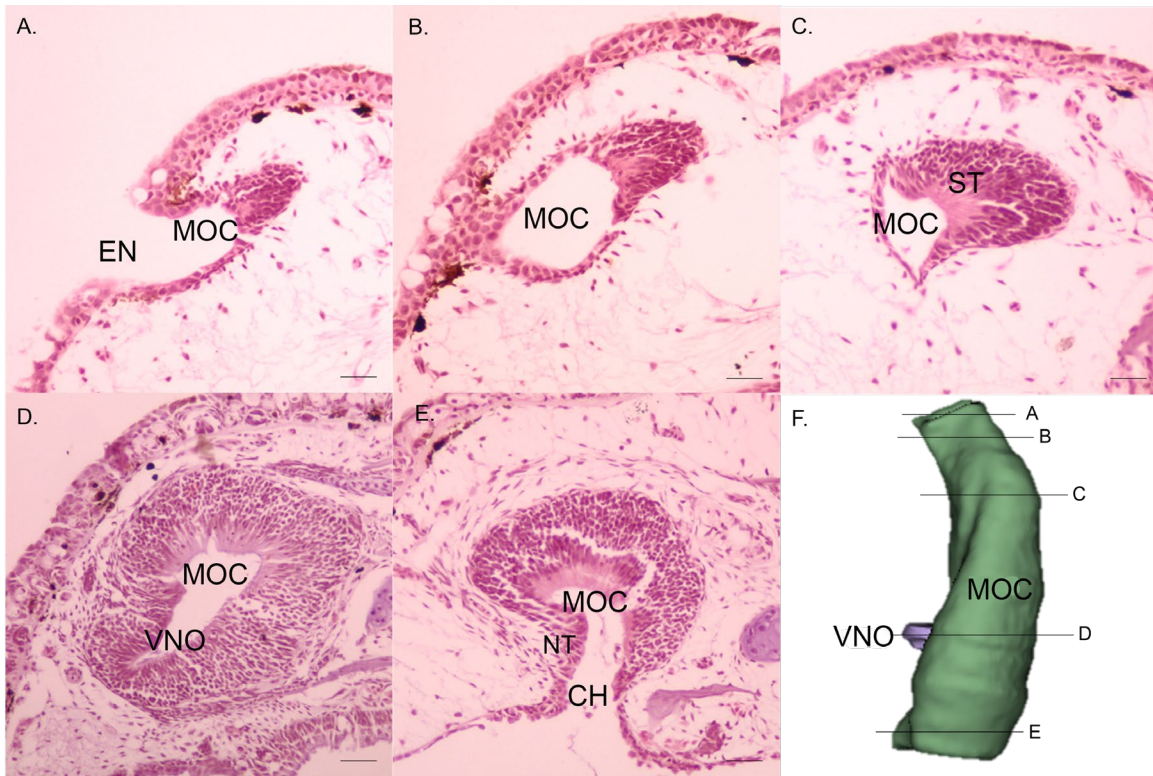
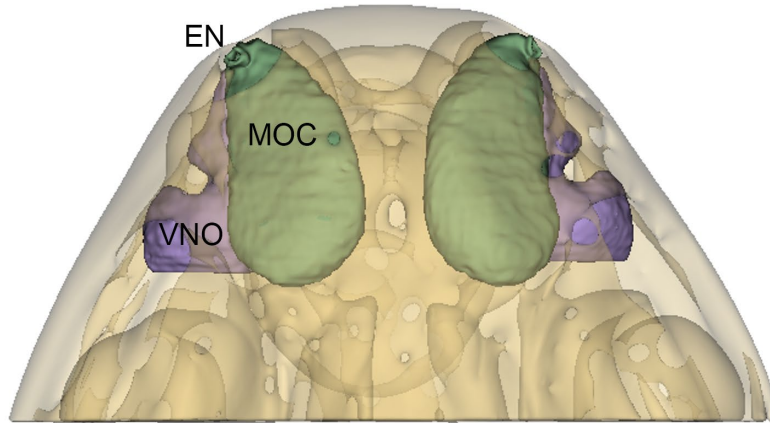


**Figure 13.** *A-E*) Histological sections of larval “*E. bislineata*” taken transversely through the nasal cavity from anterior to posterior, showing the external naris (EN), main olfactory cavity (MOC), vomeronasal organ (VNO), choana (CH), sensory tissue (ST), and nonsensory tissue (NT). *F*) 3D reconstruction with approximate section locations. Scale bar = 0.25 mm.

The MOC of adult “*E. bislineata*” is similar to that of other non-paedomorphic adults, with the olfactory tissue extending anterior to the external naris (Figs. 14 and 15). The sensory tissue is distributed throughout the MOC and VNO. It is thickest in the anterior portion of the MOC and VNO (Figs. 15A- 15D). At the choana the sensory tissue has largely been replaced by nonsensory tissue (Fig. 15E). The VNO extends laterally twice (Fig. 14), creating a two-lobed appearance like that seen in the adult *G. porphyriticus*.

A.



B.

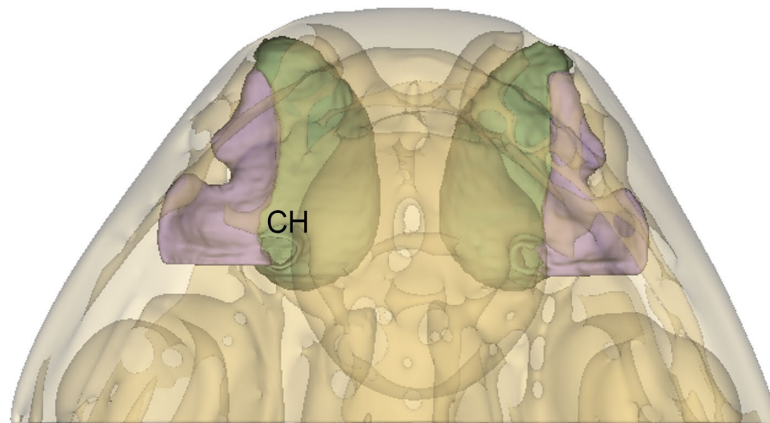


**Figure 14.** 3D reconstruction of adult “*E. bislineata*” showing the MOC (green), VNO (purple), external naris (EN), and choana (CH). Dorsal (A) and ventral (B) view. Scale bar = 0.44 cm.

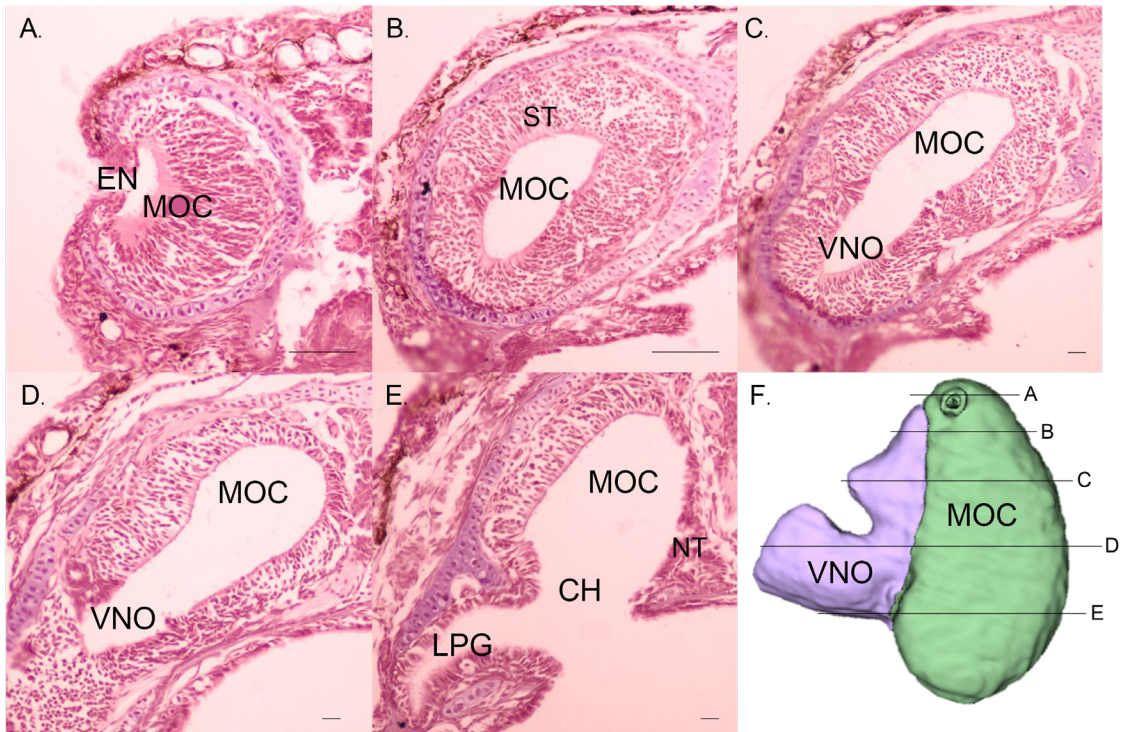
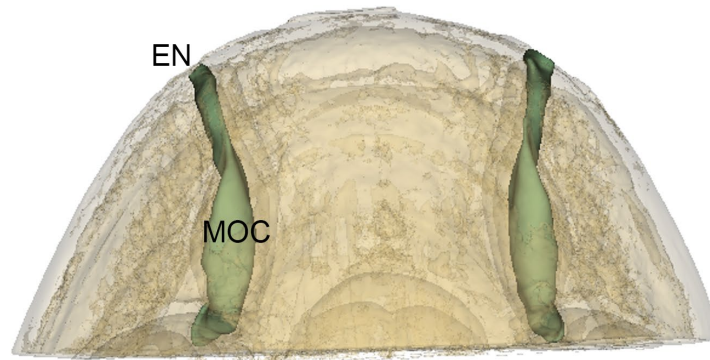


**Figure 15.** *A-E*) Histological sections of adult “*E. bislineata*” taken transversely through the nasal cavity from anterior to posterior, showing the external naris (EN), main olfactory cavity (MOC), vomeronasal organ (VNO), lateral palatal groove (LPG), choana (CH), sensory tissue (ST), and nonsensory tissue (NT) *F*) 3D reconstruction with approximate section locations. Scale bar = 0.5 mm.

### *Eurycea troglodytes*

The structure of the MOC and VNO of paedomorphic adult *E. troglodytes* is similar to that seen in the aquatic larval stages of other species. The MOC begins at the external naris and extends posteriorly as a narrow tube with the VNO being a small lateral projection (Figs. 16 and 17). The sensory epithelium in the anterior MOC is confined to the medial wall (Fig. 17B), but more posteriorly it is distributed throughout the MOC (Figs. 17C and 17D). The sensory tissue of the MOC extends back to the choana, where it is thickest along the roof, however at this point the walls are lined with nonsensory tissue (Fig. 17E).

A.



B.

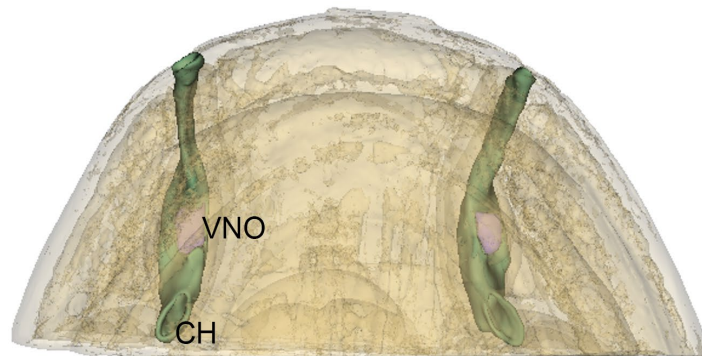


**Figure 16.** 3D reconstruction of *E. troglodytes* showing the MOC (green), VNO (purple), external naris (EN), and choana (CH). Dorsal (A) and ventral (B) view. Scale bar = 0.07 cm.

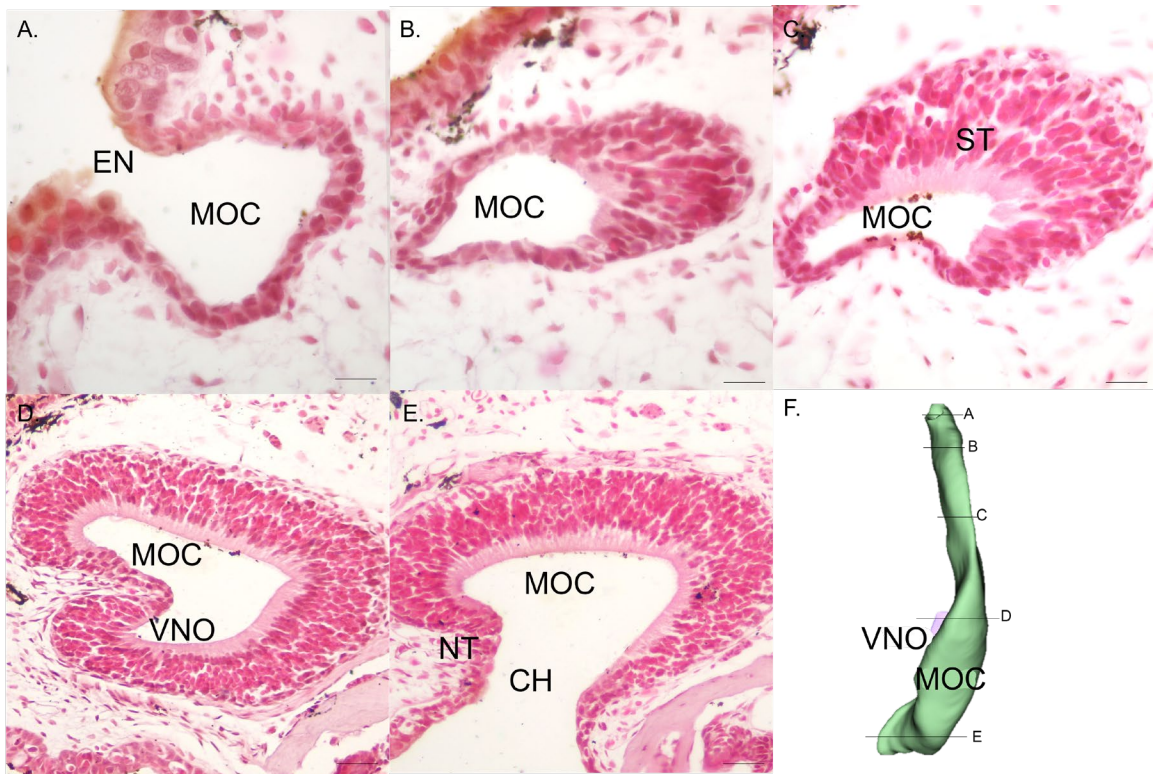


**Figure 17. A-E)** Histological sections of adult *E. troglodytes* taken transversely through the nasal cavity from anterior to posterior, showing the external naris (EN), main olfactory cavity (MOC), vomeronasal organ (VNO), choana (CH), sensory tissue (ST), and nonsensory tissue (NT). **F)** 3D reconstruction with approximate section locations. Scale bar = 0.25 mm.

## Ultrastructure of cell types

*Rhyacotriton variegatus*

The MOC of larval *R. variegatus* shows ciliated receptor cells (Rc), microvillar receptor cells (Rm), and secretory supporting cells (Sv) (Fig. 18). Secretory supporting cells are the most common cell type, a condition also seen in other species in this study. Microvillar receptor cells are less prevalent than the other two cell types seen, but not uncommon.

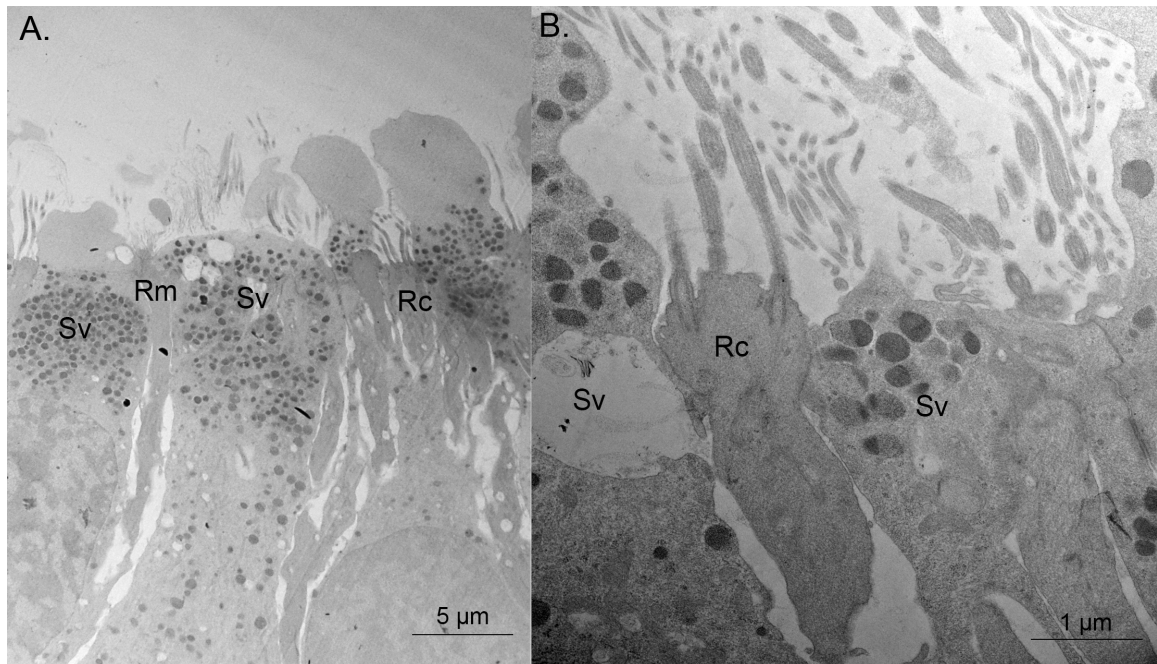


**Figure 18.** Micrographs of the ultrastructure of the MOC in larval *R. variegatus* showing ciliated receptor cells (Rc), microvillar receptor cells (Rm), and secretory supporting cells (Sv). Note that the secretory vesicles are electron-dense. The large gaps between cells (A) are commonly seen more posteriorly in the MOC.

In the VNO of larval *R. variegatus*, all four cell types are present: ciliated receptor cells, microvillar receptor cells, secretory supporting cells, and ciliated supporting cells (Fig. 19). No cell type is noticeably more common than the others.

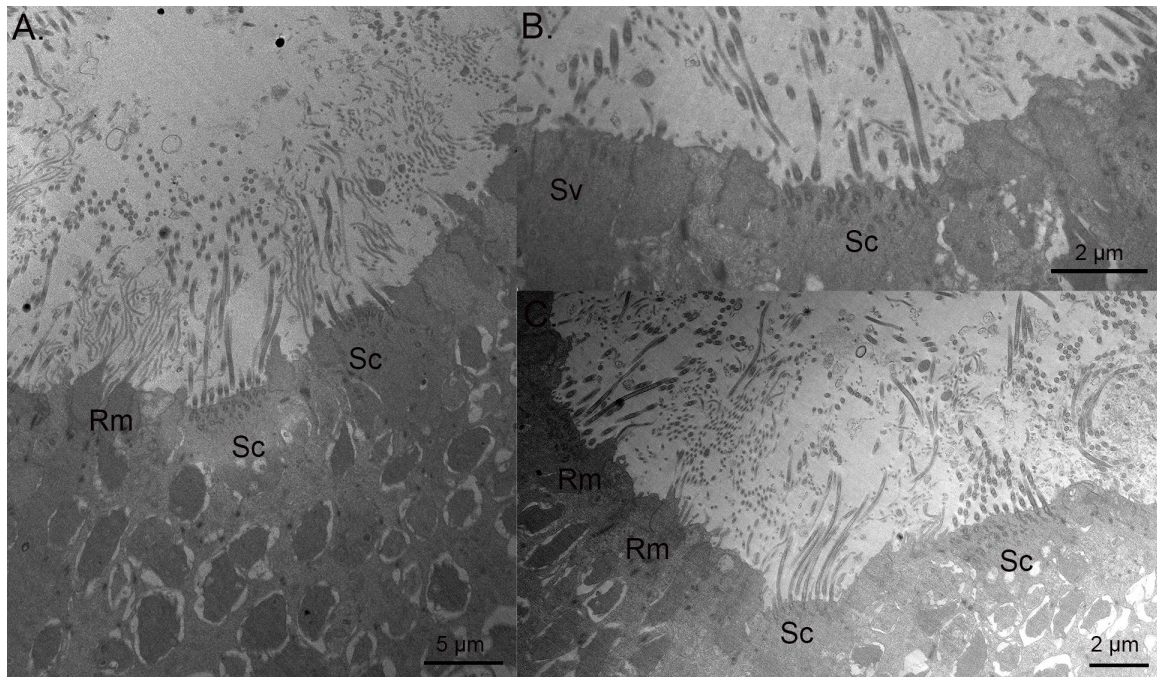


**Figure 19.** Micrographs of the ultrastructure of the VNO in larval *R. variegatus* showing microvillar receptor cells (*Rm*), ciliated supporting cells (*Sc*), and secretory supporting cells (*Sv*).

In contrast to the larval condition, in the MOC of adult *R. variegatus* only ciliated receptor cells and secretory supporting cells are present. The cells appear to be in an alternating pattern with one type following the other (Fig. 20). This is a pattern that is also seen in the MOC of other terrestrial adults in this study.

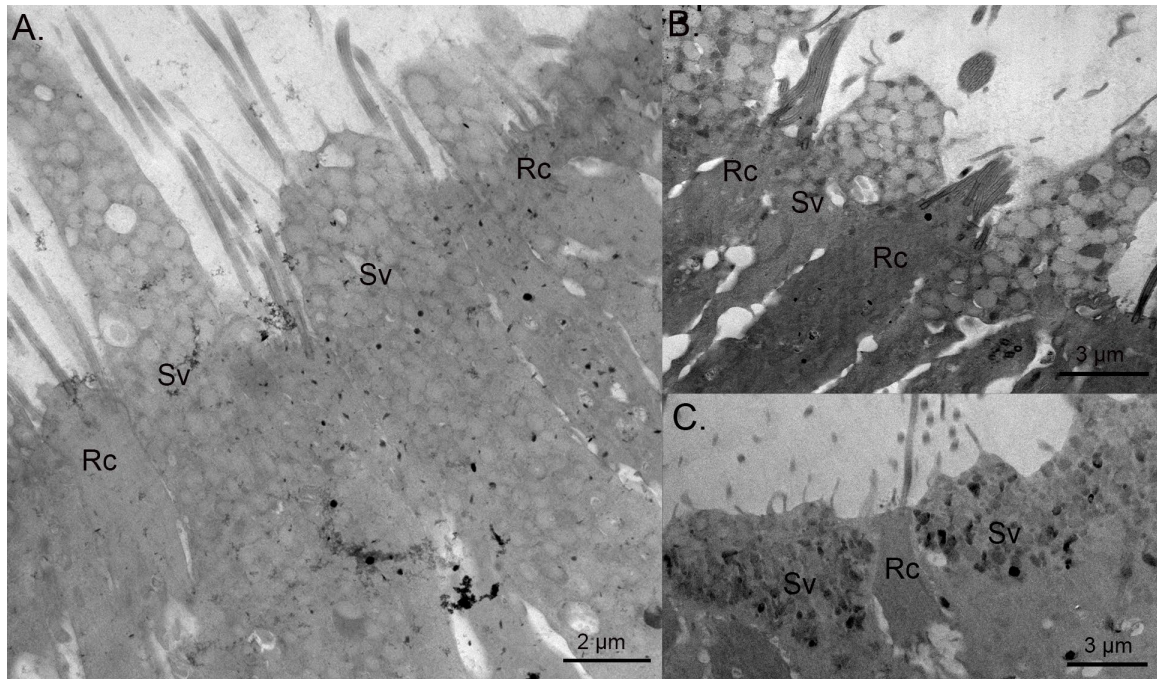


**Figure 20.** Micrographs of the ultrastructure of the MOC in adult *R. variegatus* showing ciliated receptor cells (Rc) and secretory supporting cells (Sv). Notice the presence of both electron-lucent (A) and electron-dense (C) vesicles.

The VNO of adult *R. variegatus* has microvillar receptor cells (Rm), secretory supporting cells (Sv), and ciliated supporting cells (Sc). Ciliated supporting cells are the most common cell type observed. They are also much larger relative to the other two cell types present in the VNO (Fig. 21B).

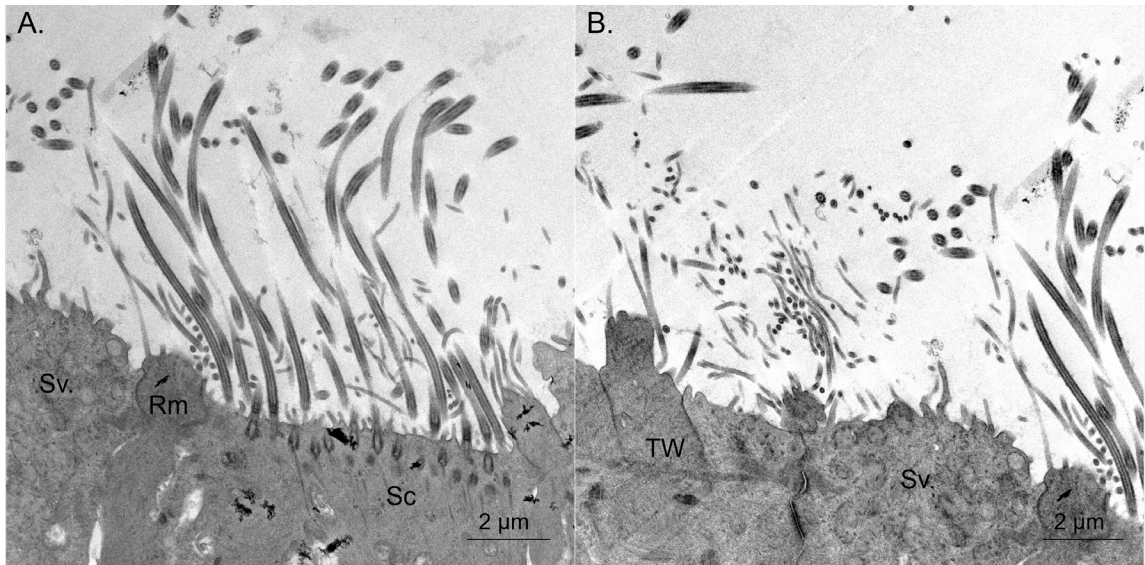


**Figure 21.** Micrographs of the ultrastructure of the VNO in adult *R. variegatus* showing microvillar receptor cells (Rm), ciliated supporting cells (Sc), and secretory supporting cells (Sv). Note the terminal web (TW) present in the supporting cells (**B**).

*Batrachoseps attenuatus*

The MOC of *B. attenuatus* contains only ciliated receptor cells and secretory supporting cells. The cells have an alternating arrangement (Fig. 22) similar to that seen in the MOC of adult *R. variegatus*.

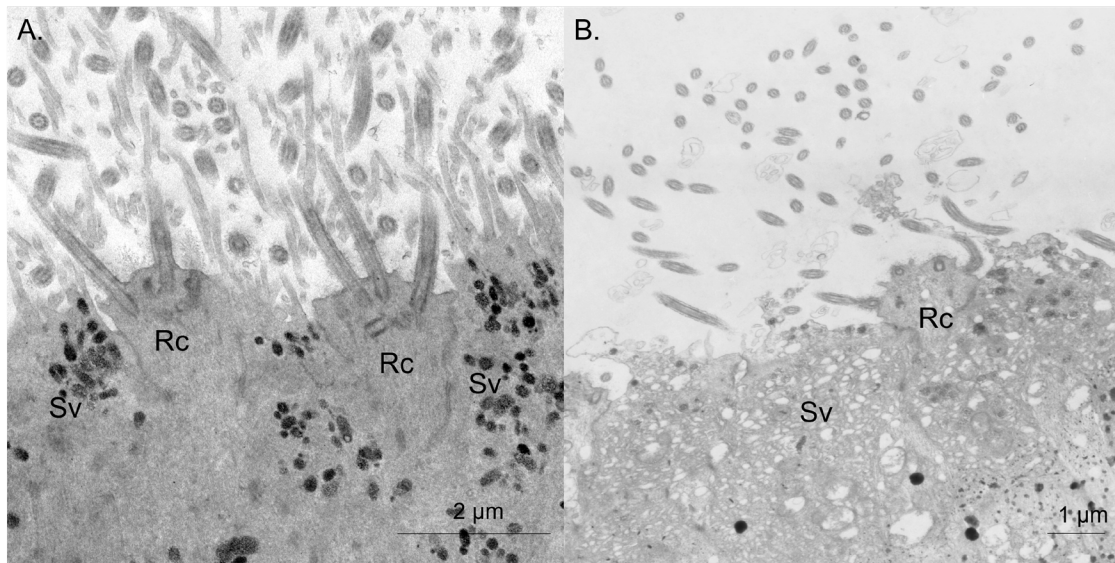


**Figure 22.** Micrographs of the ultrastructure of the MOC in adult *B. attenuatus* showing ciliated receptor cells (Rc) and secretory supporting cells (Sv). Notice the presence of both electron-lucent (B) and electron-dense secretory vesicles (A).

The VNO of *B. attenuatus* contains all four cell types: ciliated receptor cells, microvillar receptor cells, secretory supporting cells, and ciliated supporting cells (Fig. 23). Ciliated receptor cells and secretory supporting cells are most common.

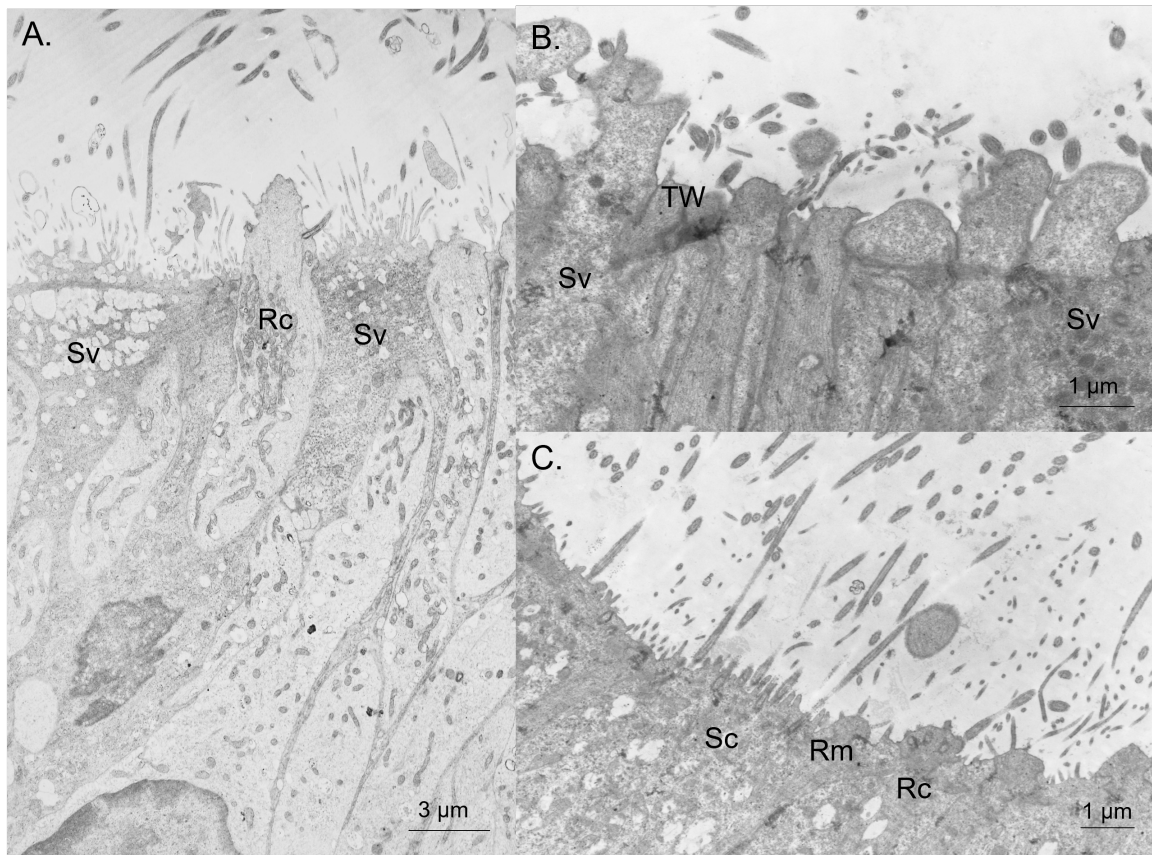


**Figure 23.** Micrographs of the ultrastructure of the VNO in adult *B. attenuatus* showing ciliated receptor cells (Rc), microvillar receptor cells (Rm), ciliated supporting cells (Sc), and secretory supporting cells (Sv). Note the terminal web (TW) in the supporting cells (B) and the electron-lucent vesicles in the supporting cells (C).

*Gyrinophilus porphyriticus*

In the MOC of larval *G. porphyriticus* all four cell types are present: ciliated receptor cells, microvillar receptor cells, ciliated supporting cells, and secretory supporting cells (Fig. 24). Ciliated receptor cells and secretory supporting cells are the most common cell types in the MOC.

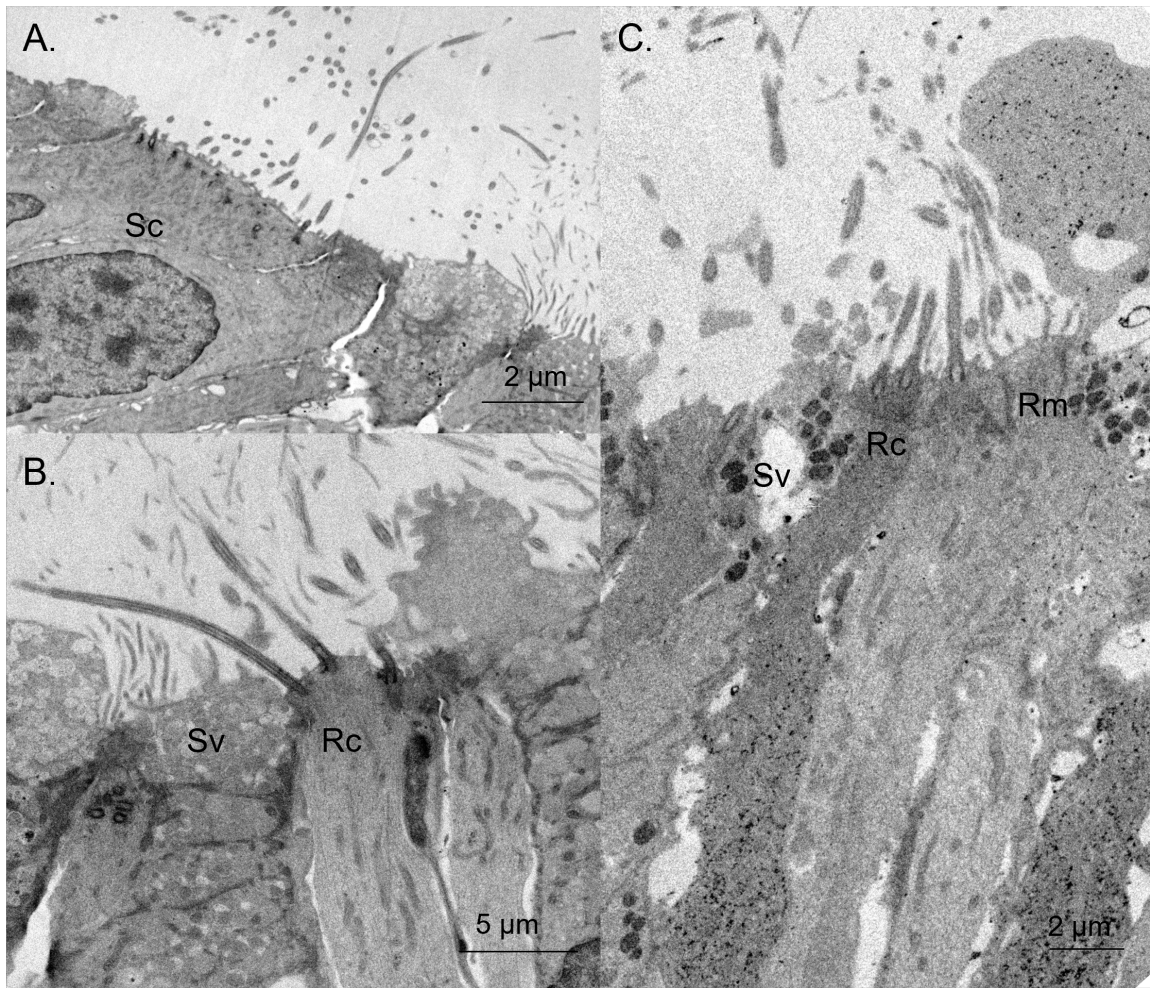


**Figure 24.** Micrographs of the ultrastructure of the MOC in larval *G. porphyriticus* showing ciliated receptor cells (Rc), microvillar receptor cells (Rm), ciliated supporting cells (Sc), and secretory supporting cells (Sv).

The VNO of larval *G. porphyriticus* also has all four cell types: ciliated receptor cells, microvillar receptor cells, ciliated supporting, and secretory supporting cells (Fig. 25). Ciliated receptor cells are less common than the other cell types.

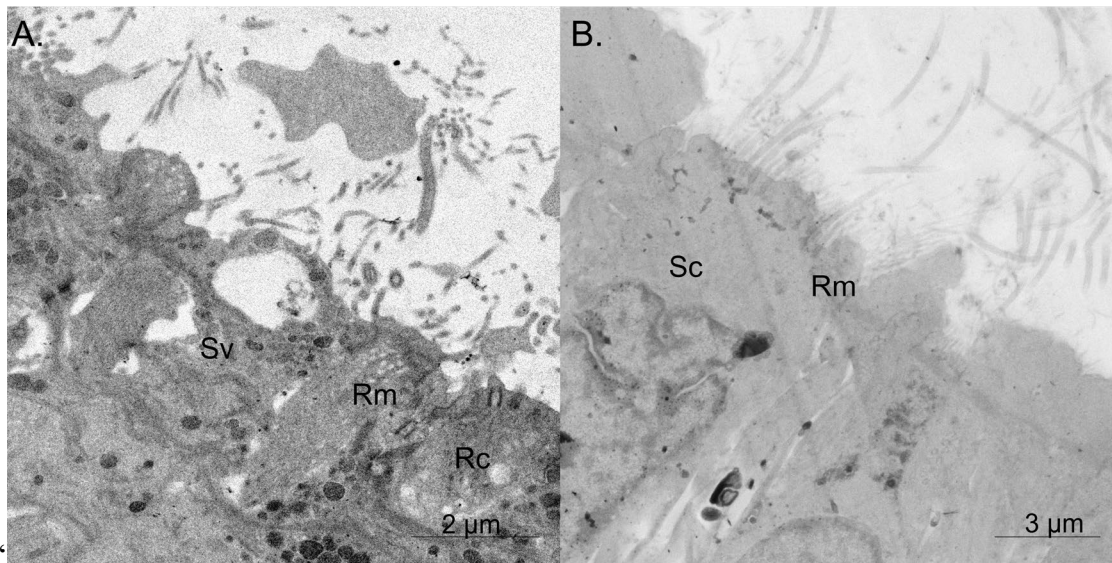


**Figure 25.** Micrographs of the ultrastructure of the VNO in larval *G. porphyriticus* showing ciliated receptor cells (*Rc*), microvillar receptor cells (*Rm*), and secretory supporting cells (*Sv*), and ciliated supporting cells (*Sc*).

As in the larva, in the MOC of adult *G. porphyriticus* all four cell types are present. Ciliated receptor cells and secretory supporting cells are the most common and appear in an alternating arrangement (Figs. 26B and 26C), which gives the MOC a similar overall appearance to the MOC of adult *R. variegatus* and *B. attenuatus*.

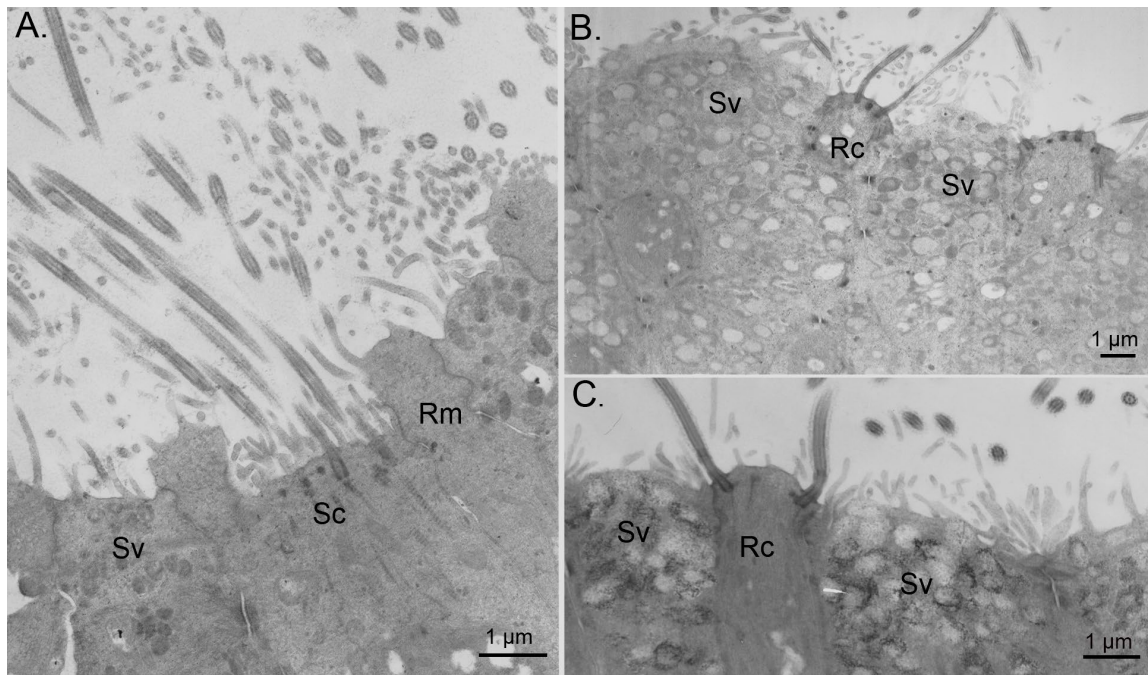


**Figure 26.** Micrographs of the ultrastructure of the MOC in adult *G. porphyriticus* showing ciliated receptor cells (Rc), microvillar receptor cells (Rm), ciliated supporting cells (Sc), and secretory supporting cells (Sv). Notice the electron-dense secretory vesicles (A) in comparison to the electron-lucent vesicles (B and C).

The VNO of adult *G. porphyriticus* also resembles that of the larva: all four cell types are present: ciliated receptor cells, microvillar receptor cells, ciliated supporting cells, and secretory supporting cells. All cell types appear in approximately equal abundance (Fig. 27).

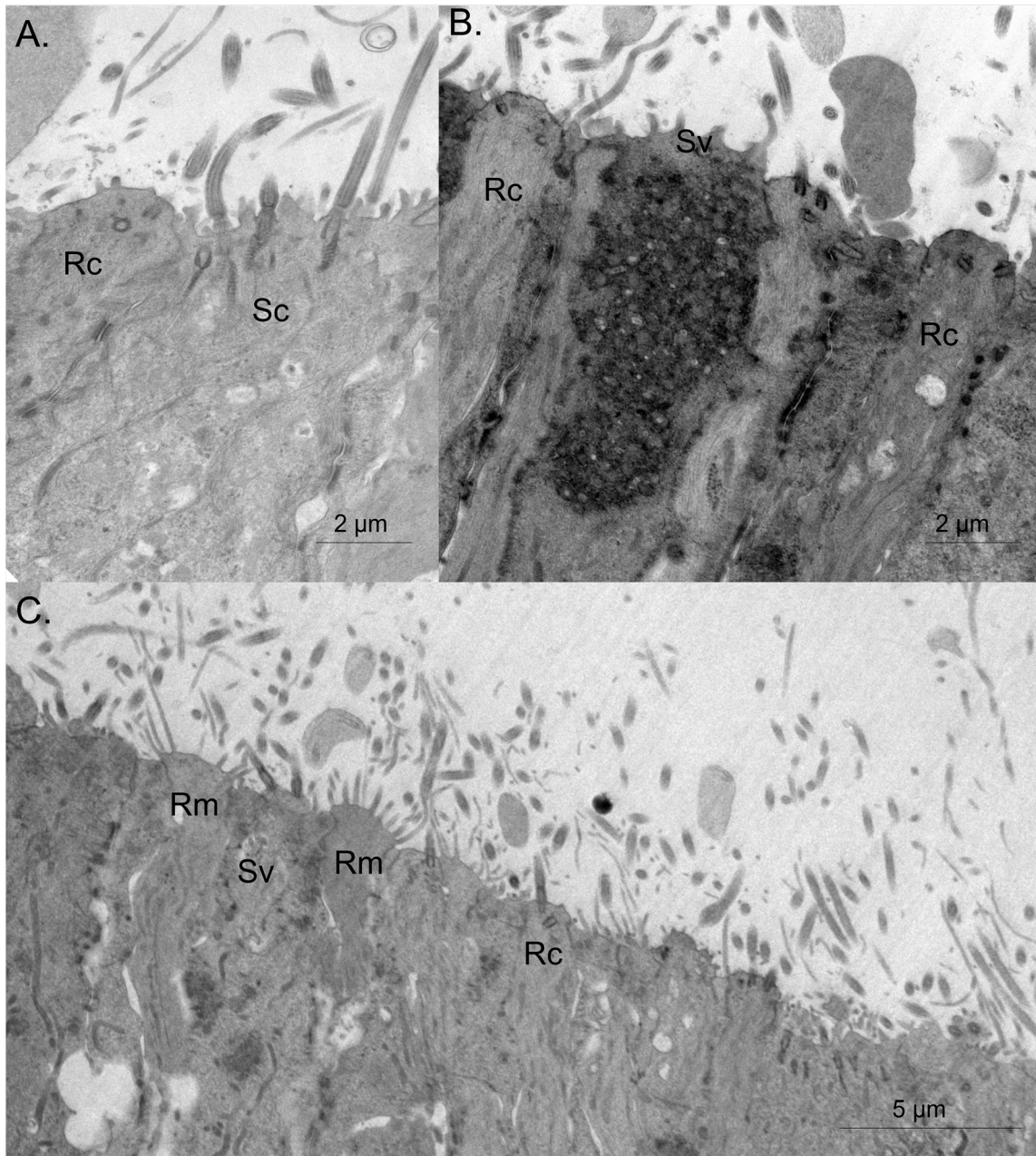


**Figure 27.** Micrographs of the ultrastructure of the VNO in adult *G. porphyriticus* showing ciliated receptor cells (Rc), microvillar receptor cells (Rm), ciliated supporting cells (Sc), and secretory supporting cells (Sv).

“Eurycea bislineata”

In the MOC of larval “*E. bislineata*” ciliated receptor cells, microvillar receptor cells, and secretory supporting cells are present (Fig. 28). All three cell types are about equally abundant.

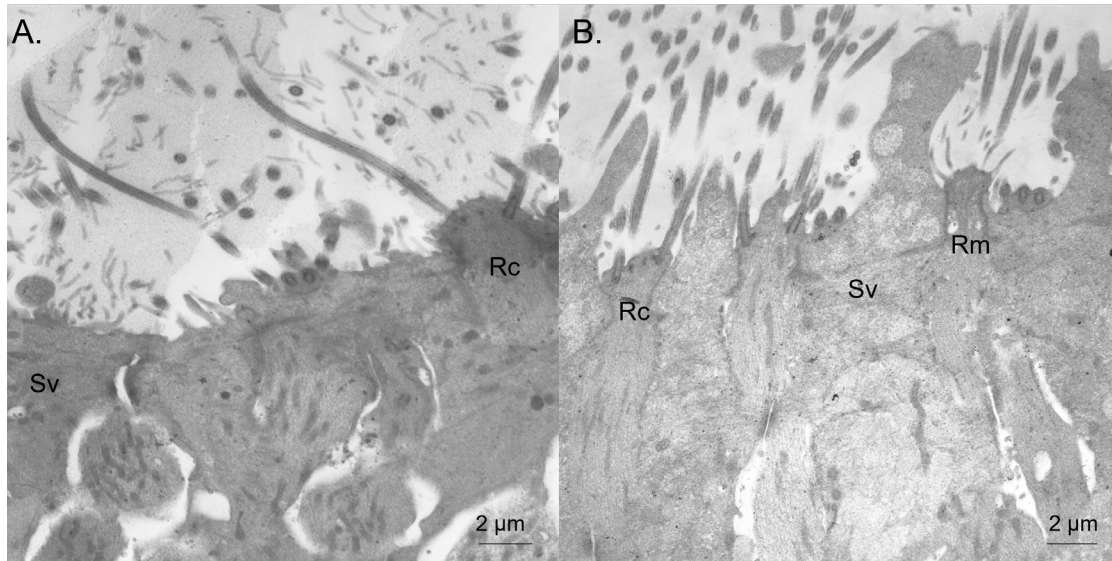


**Figure 28.** Micrographs of the ultrastructure of the MOC in larval “*E. bislineata*” showing ciliated receptor cells (Rc), microvillar receptor cells (Rm), and secretory supporting cells (Sv). Notice the secretory vesicles are electron-dense. Notice the irregular arrangement of the cells, with large spaces between them (A) in the posterior region of the MOC, compared to the regularly arranged cells (B) in the anterior portion of the MOC.

In the larval “*E. bislineata*” VNO all four cell types are present (Fig. 29) and all cell types are about equally abundant.

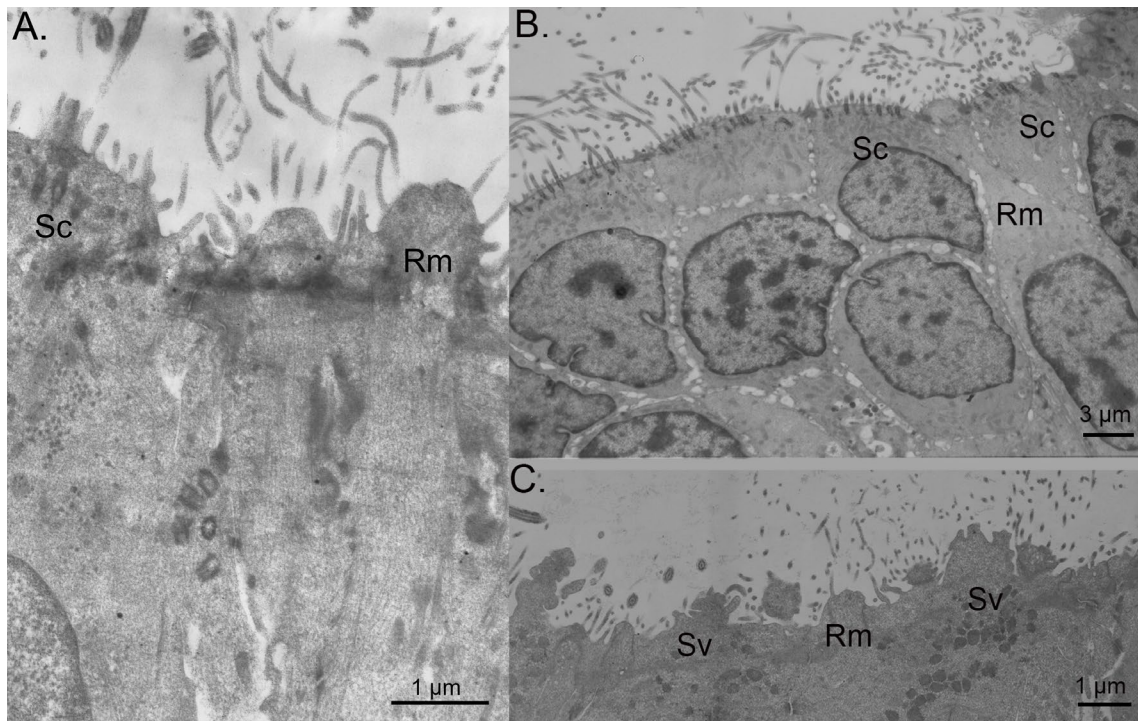


**Figure 29.** Micrographs of the ultrastructure of the VNO in larval “*E. bislineata*” showing microvillar receptor cells (Rm), secretory supporting cells (Sv), ciliated receptor cells (not pictured) and supporting cells (Sc). Notice the arrangement of the nuclei in (B), with the supporting cells having more apical nuclei and the receptor cells having more basal nuclei.

In contrast to the larva, in the MOC of adult “*E. bislineata*” all four cell types are present: ciliated receptor cells, microvillar receptor cells, ciliated supporting cells, and secretory supporting cells (Fig. 30). All cell types are about equally abundant.

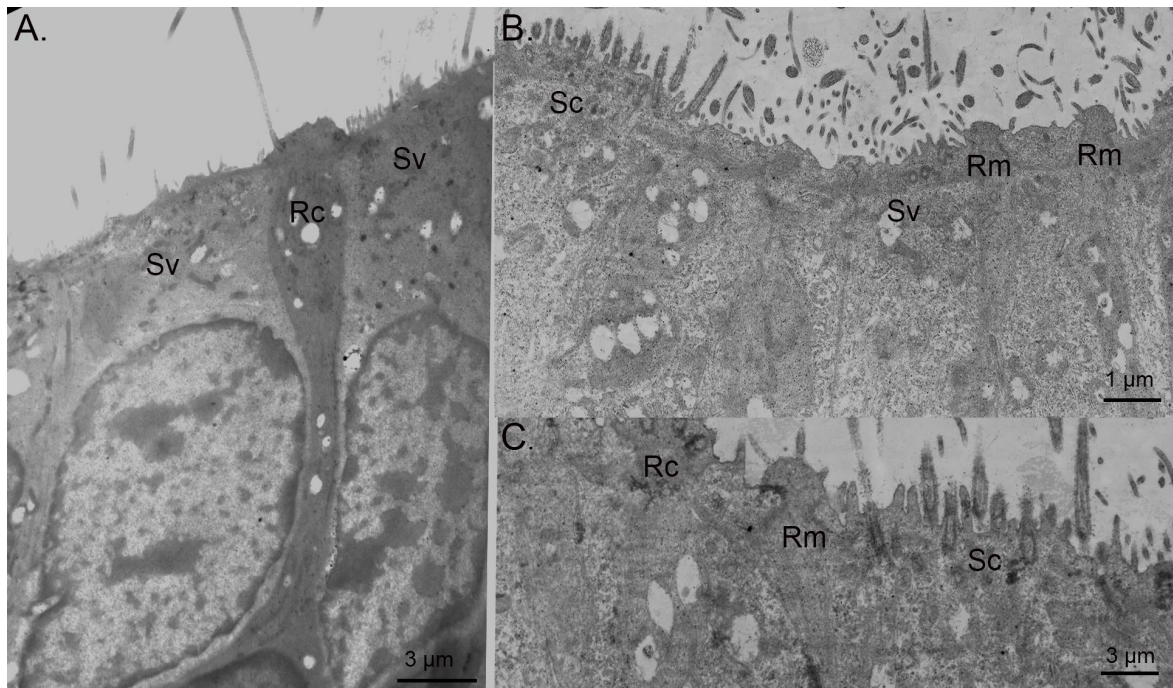


**Figure 30.** Micrographs of the ultrastructure of the MOC in adult “*E. bislineata*” showing ciliated receptor cells (Rc), microvillar receptor cells (Rm), ciliated supporting cells (Sc), and secretory supporting cells (Sv). Notice the location of the nuclei (A) with the supporting cells having more apical nuclei and the receptor cells having more basal nuclei. Note the electron-lucent secretory vesicles (B and C).

In the VNO of adult “*E. bislineata*”, like the larva, all cell types are present: ciliated receptor cells, microvillar receptor cells, ciliated supporting cells, and secretory supporting cells (Fig. 31). All cell types are about equally common.

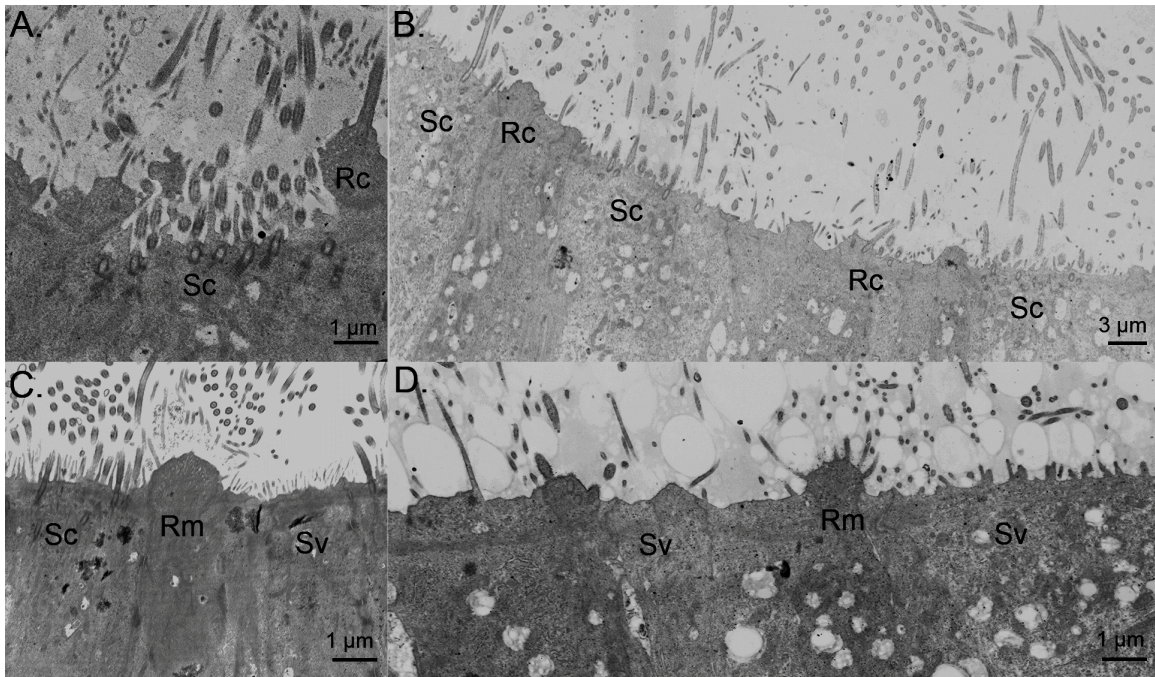


**Figure 31.** Micrographs of the ultrastructure of the VNO in adult “*E. bislineata*” showing ciliated receptor cells (Rc), microvillar receptor cells (Rm), ciliated supporting cells (Sc), and secretory supporting cells (Sv). Notice the secretory vesicles are electron-lucent.

*Eurycea troglodytes*

In the MOC of the paedomorphic adults of *E. troglodytes* I found ciliated receptor cells, microvillar receptor cells, and secretory supporting cells present (Fig. 32). All cell types are about equally abundant.

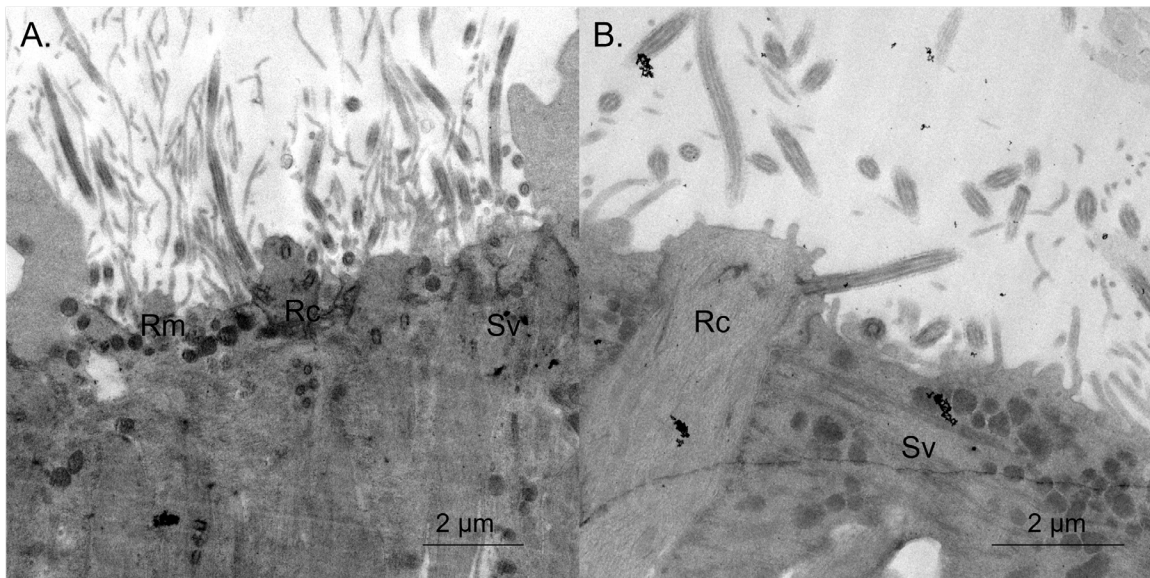


**Figure 32.** Micrographs of the ultrastructure of the MOC in *E. troglodytes* showing ciliated receptor cells (Rc), microvillar receptor cells (Rm), and secretory supporting cells (Sv).

In the VNO of *E. troglodytes* pedomorphic adults, all four cell types are present: ciliated receptor cells, microvillar receptor cells, ciliated supporting cells, and secretory supporting cells (Fig. 33). All cell types appeared to be in approximately equal abundance.

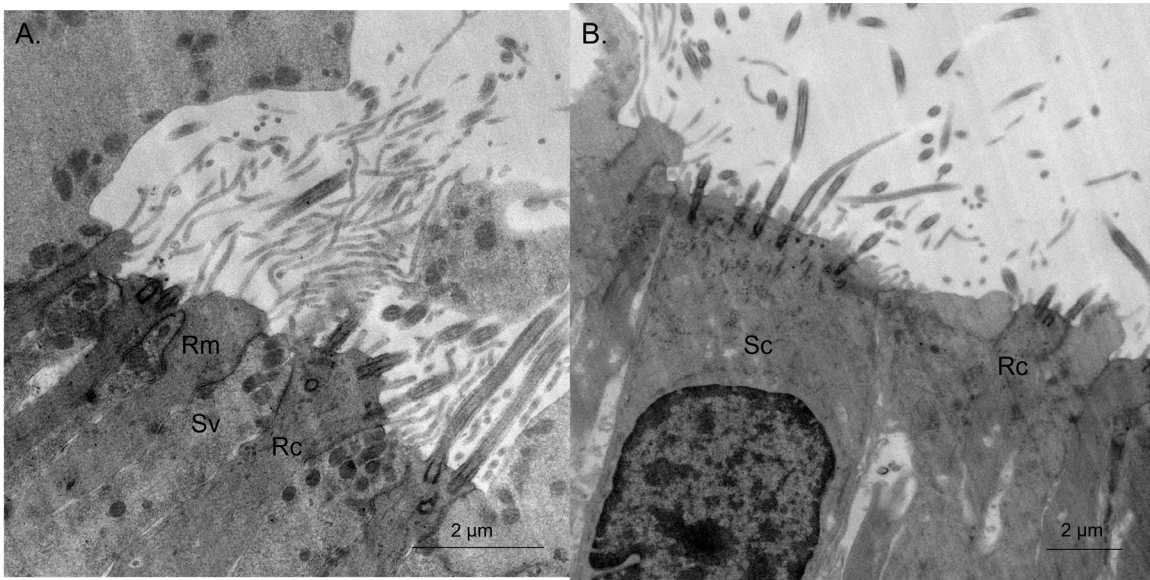


**Figure 33.** Micrographs of the ultrastructure of the VNO in *E. troglodytes* showing ciliated receptor cells (Rc), microvillar receptor cells (Rm), ciliated supporting cells (Sc), and secretory supporting cells (Sv).

## DISCUSSION

My research focused on comparing the gross morphology and cell ultrastructure of the olfactory organ of four plethodontid species and one outgroup. By comparing species with different life histories, I was able to make qualitative descriptions of similarities and differences in the MOC and VNO and draw inferences about the stasis and diversification of these parts of the olfactory system.

### Gross morphology of the MOC

At the level of gross morphology, the structure of the nose was generally consistent across all my studied species between terrestrial and aquatic morphology, including my outgroup, *R. variegatus*. However, it differed significantly between larvae and paedomorphic adults, on the one hand, and among non-paedomorphic adults, on the other.

In the plethodontid larvae examined (as well as in adults of *E. troglodytes*, a paedomorphic species), the MOC is tubular, running from external naris to choana. The epithelium of the MOC lacks ridges and is smooth and continuous. In contrast, the MOC of other larval and paedomorphic caudates, while likewise tubular, contains ridges of nonsensory epithelium, with valleys lined with sensory olfactory epithelium, which is even the case in *Amphiuma tridactylum* (in the family Amphiumidae, the sister group to Plethodontidae) (Eisthen, 2000; Reiss & Eisthen, 2008; Stuelpnagel & Reiss, 2005). In my study species, I found that the sensory olfactory epithelium is concentrated in the

anterior portion of the MOC near the external naris and is replaced by nonsensory epithelium in the posterior portion near the choana. In particular, sensory epithelium at the choana is concentrated along the roof of the MOC, and the walls are lined with nonsensory epithelium. This is opposite to the MOC of both the larval and neotenic *D. tenebrosus*, in which the anterior portion of the olfactory cavity is nonsensory and the sensory epithelium begins after a nonsensory vestibule and persists in the MOC through the choana (Stuelpnagel & Reiss, 2005).

The MOCs of the (non-paedomorphic) adults of the outgroup species *R. variegatus* and of the plethodontids I examined are most similar to the more terrestrial plethodontid species (genera *Plethodon* and *Bolitoglossa*) described by Dawley (2017). In all these species, the MOC begins slightly anterior to the external naris and extends posteriorly, forming a sac-like shape. This differs from the tubular shape of the MOC in the larval and paedomorphic condition. The tissue at the posterior region of the MOC (near the choana) is nonsensory compared to that of the larvae, where some sensory tissue remains on the roof of the MOC. This is the same condition that was observed in other plethodontid species (Dawley, 2017). Dawley (2017) suggests that the thickness of the epithelium in the anterior MOC may maximize the detection of aerial odorants that enter through the external naris.

### Gross morphology of the VNO

Consistent with previous studies, the VNO of the taxa of the species varied greatly across life stages. In larval *R. variegatus*, *G. porphyriticus* and “*E. bislineata*,”

and in paedomorphic *E. troglodytes*, the VNO is a relatively small lateral diverticulum off the MOC, similar to that described for larvae of other caudate species, especially *D. tenebrosus* (Stuelpnagel & Reiss, 2005). The larval VNO is largely populated by sensory epithelium with very little nonsensory epithelium. By contrast, the shape of the VNO in metamorphosed adults varied across species in this study, with the VNO of *R. variegatus* and *B. attenuatus* having just one lateral extension and the VNO of *G. porphyriticus* and “*E. bislineata*” having two lateral extensions, creating a two-lobed shape. Dawley and Bass (1988) also found a two-lobed shape in *Plethodon cinereus*, a fully terrestrial, direct developing species. Despite the shape of the VNO, the vomeronasal sensory epithelium of plethodontid species was consistent in that it was thickest at the anterior portion of the VNO and became thinner and replaced by nonsensory tissue in the posterior portion. However, in *R. variegatus* the epithelium in the posterior portion was much thicker than that of the plethodontid species. Dawley and Bass (1988) proposed that the vomeronasal sensory epithelium in plethodontids has shifted anteriorly compared to that of other families in tandem with the function of the nasolabial grooves, which plethodontids use to transport nonvolatile odorants to the VNO. This anterior transition of sensory epithelium in plethodontids likely reflects enhanced odorant delivery to the VNO compared to other salamander families.

The influence of phylogeny, environment, and life history on olfactory cell types

Despite much research done on the olfactory system of salamanders, no previous studies have been done on a phylogenetically restricted group of species to determine the

relationship of phylogeny, environment, and life history to olfactory cell types. By looking at closely related species with varying life history strategies in Plethodontidae I was able to determine the cell types present in the MOC and VNO and compare those to the phylogeny, environment, and life history of the species.

Variation in cell types in the MOC across species and life history stages is considerable. I found little support in the MOC for my prediction that olfactory organization is consistent across species with the same life history strategy. The MOC of larval *R. variegatus*, *G. porphyriticus*, and "*E. bislineata*," and paedomorphic *E. troglodytes*, contains ciliated receptor cells, microvillar receptor cells, and secretory supporting cells (Table 2, Fig 34). These three cell types are also present in the paedomorphic amphiumid *A. tridactylum* (Amphiumidae is the sister group to Plethodontidae)(Eisthen, 2000). This cell type composition closely resembles that of some previously studied aquatic caudates (larvae and paedomorphs). But environment and life history stage are not strictly correlated with cell type: in the larva of *G. porphyriticus* these three cell types are additionally accompanied by ciliated supporting cells, which is the cellular composition observed in the larval MOC of *D. tenebrosus* (Stuelpnagel & Reiss, 2005).

**Table 2.** Comparison of previous work on cell types in the amphibian olfactory epithelium with results of the present study: Rc, ciliated receptor cell; Rm, microvillar receptor cell; Sv, secretory supporting cell; Sc, ciliated supporting cell. General caudate cell types are informed by studies based on several families including Proteidae, Sirenidae, Amphiumidae, Dicamptodontidae, and Salamandridae. Parentheses indicate the presence in some but not all families (Benzekri & Reiss, 2012; Eisthen, 2000; Stuelpnagel & Reiss, 2005).

Species or group	Cell types present in MOC	Cell types present in VNO
Anurans (general)	Sc, Sv, Rc, Rm (aquatic larva)	Sc, Rm
	Sv, Rc (terrestrial adult)	
Caudates (general)	(Sc), Sv, Rc, Rm (aquatic larva)	Sc, Sv, Rm or
	Sv, Rc, Rm (terrestrial adult)	Sv, Rc, Rm
<i>R. variegatus</i>	Sv, Rc, Rm (larva)	Sc, Sv, Rm
	Sv, Rc (adult)	
<i>B. attenuatus</i>	Sv, Rc (adult)	Sc, Sv, Rc, Rm
<i>G. porphyriticus</i>	Sc, Sv, Rc, Rm (larva & adult)	Sc, Sv, Rc, Rm
“ <i>E. bislineata</i> ”	Sv, Rc, Rm (larva)	Sc, Sv, Rc, Rm
	Sc, Sv, Rc, Rm (adult)	
<i>E. troglodytes</i>	Sv, Rc, Rm (paedomorph)	Sc, Sv, Rc, Rm

That larval “*E. bislineata*” and paedomorphic adult *E. troglodytes* would closely resemble each other in terms of ultrastructure is logical due to their close phylogenetic relationship (Bonett et al., 2014b) and similar habitats. However, they are more similar in ultrastructure to larval *R. variegatus* than to larval *G. porphyriticus*. This is unexpected because the habitat of larvae of all of these species is similar, and *Gyrinophilus* and *Eurycea* are more closely related to each other than to *Rhyacotriton* (Pyron & Wiens, 2011; Shen et al., 2016).

In the MOC of terrestrial stages, including adults of biphasic *R. variegatus* and direct developing *B. attenuatus*, only ciliated receptor cells and secretory supporting cells

are always present (Table 2, Fig. 35). These two cell types are additionally accompanied by ciliated supporting cells and microvillar receptor cells in adult *G. porphyriticus* and “*E. bislineata*”. The condition of the MOC of *B. attenuatus* and adult *R. variegatus*, with only secretory supporting cells and ciliated receptor cells, resembles the anuran “adult type” epithelium that is used for aerial olfaction (Benzekri & Reiss, 2012). Both of these are terrestrial life stages of these species, however *R. variegatus* is much more aquatic than *B. attenuatus*, seldom being found far from a stream, and returning to seep habitats to reproduce (Doten et al., 2017). This habitat preference suggests that *R. variegatus* might also have regions of “larval type” epithelium present in the MOC in addition to the “adult type”, as is the case in *D. tenebrosus* (Stuelpnagel & Reiss, 2005). However, I found no evidence of this type of epithelium in the sections I examined.

The MOC of adult *G. porphyriticus* and adult “*E. bislineata*”, which contains all four cell types (ciliated receptor cells, microvillar receptor cells, ciliated supporting cells, and secretory supporting cells), is similar to the ultrastructure associated with aquatic olfaction in anurans and larval *D. tenebrosus* (Benzekri & Reiss, 2012; Stuelpnagel & Reiss, 2005). Both *G. porphyriticus* and “*E. bislineata*” are biphasic species with fully aquatic larvae and terrestrial adults that remain near streams or seeps, which might explain this, but of course a similar life history and habitat is seen in *R. variegatus* (AmphibiaWeb, 2022a, 2022b, 2022c), which has only two cell types present in the adults, further indicating that the relationship between cell type, life history strategy, and habitat is unclear.

Secretory supporting cells and ciliated receptor cells are present in the MOC in all species and stages used for my study, a result consistent with previous studies on anurans and other caudates (Table 2; Benzekri & Reiss, 2012; Eisthen, 2000; Stuelpnagel & Reiss, 2005). In a previous study on *Ascaphus truei*, all four cell types were present in both the larval and adult MOC. However, in the adult MOC there were two distinct types of epithelia: the “larval type” which contained all four cell types, and the “adult type” which only contained ciliated supporting cells and secretory supporting cells (Benzekri & Reiss, 2012). As noted above, a similar pattern is seen in the adult *D. tenebrosus*, in which there are distinct regions of epithelia that resemble the larval MOC and regions that differ in terms of cell types (Stuelpnagel & Reiss, 2005). It was proposed that these “larval type” regions persisted in the MOC for aquatic olfaction when the adult would return to aquatic habitats to breed. In the plethodontid MOC, I found no apparent correlation between cell type and habitat. Moreover, in the present study I saw no evidence of regional specialization of the olfactory epithelium in the species I examined, although my sampling of the cavity was more extensive in some species than others.

When determining the evolution of the cell types present in the MOC it appears that the presence of ciliated receptor cells, microvillar receptor cells, and secretory supporting cells are the ancestral condition for larvae and paedomorphs within the Plethodontidae, as this condition is present in the sister taxa *Rhyacotriton* and *Amphiuma* (Fig. 34A). Ciliated supporting cells then appear only in *G. porphyriticus*. In the terrestrial adult MOC (Fig. 34B) it seems that ciliated supporting cells and secretory cells are the ancestral condition, which is logical as this is the “aerial olfaction” condition

(Benzekri & Reiss, 2012). Then in the Spelerpini clade, microvillar receptor cells and ciliated supporting cells appeared in adults as well.

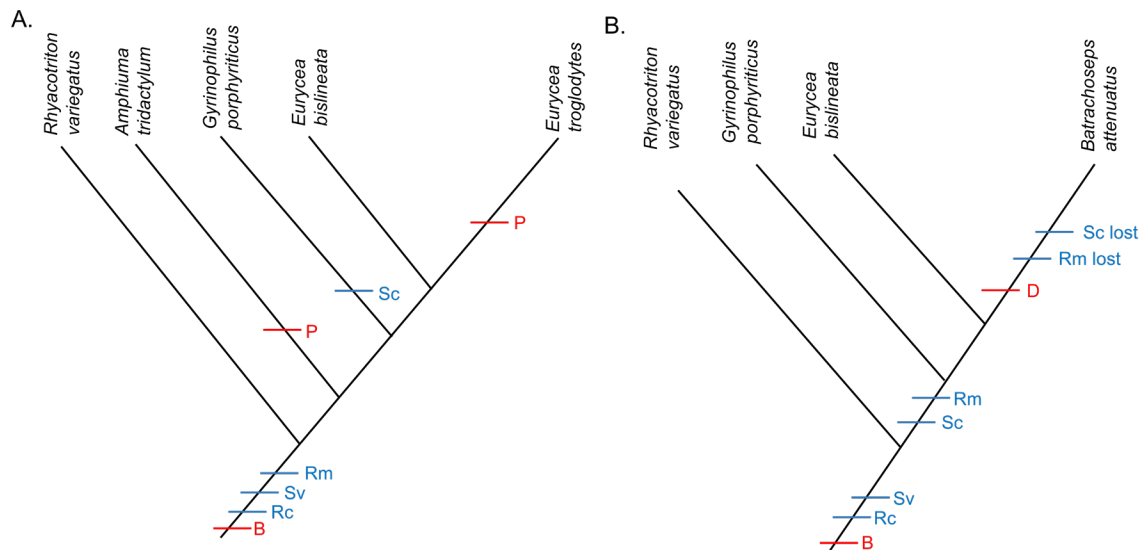


**Figure 34.** Simplified phylogeny of plethodontid salamanders and their relatives showing evolution of life history strategies (red) and cell types present in the MOC (blue). Phylogenies depict presence/absence in the MOC, not origin of cell types; it is assumed all cell types are ancestrally available. **A)** Results for larval stages of biphasic (B) species and for paedomorphic (P) species. **B)** Results for adult stages of biphasic (B) species and direct-developing (D) species (Eisthen, 2000; Pyron & Wiens, 2011; Shen et al., 2016). Rc, ciliated receptor cell; Rm, microvillar receptor cell; Sv, secretory supporting cell; Sc, ciliated supporting cell.

Turning to the VNO, we find that it shows much less variation in cell type than does the MOC. All four cell types (ciliated receptor cells, microvillar cells, ciliated supporting cells, and secretory supporting cells) are present in the VNO of all the aquatic stages and species of plethodontids I examined, including larvae of the biphasic species *G. porphyriticus* and “*E. bislineata*” and paedomorphic adults of *E. troglodytes* (Fig. 35A). The same cell types are present in the VNO of the terrestrial stages and species of

plethodontids I examined, including adults of the biphasic species *G. porphyriticus*, “*E. bislineata*,” and the direct-developer *B. attenuatus*. By contrast, in the outgroup taxon *R. variegatus* only microvillar receptor cells, ciliated supporting cells, and secretory supporting cells are present in the VNO (Fig. 35B). The paedomorphic *A. tridactylum*, more closely related to plethodontids than *Rhyacotriton*, also lacks ciliated receptor cells in the VNO (Eisthen, 2000; Pyron & Wiens, 2011; Shen et al., 2016).

Comparing across all amphibians (Table 2), we find ciliated supporting cells and microvillar receptor cells present in the VNO of all species and stages. Secretory supporting cells or ciliated receptor cells are also present in the VNO of all caudates (Benzekri & Reiss, 2012; Dawley & Bass, 1989). However, only in plethodontids are all four cell types present in all life stages and species in the VNO. This result is surprising because in other caudates it is most common to see ciliated supporting cells and microvillar receptor cells accompanied by *either* ciliated receptor cells *or* secretory supporting cells. However, one aspect of the VNO of plethodontids and *R. variegatus* is consistent with previous research: in all previously studied amphibian species, the ultrastructure of the VNO remains unchanged during metamorphosis (Benzekri & Reiss, 2012; Eisthen, 2000; Stuelpnagel & Reiss, 2005).

When determining the evolution of cell types in both the larval and adult VNO it appears that microvillar receptor cells, secretory supporting cells, and ciliated supporting cells are the ancestral condition as these are present in the sister taxa (Fig. 35A, B). Ciliated receptor cells then appeared in the VNO in family Plethodontidae.

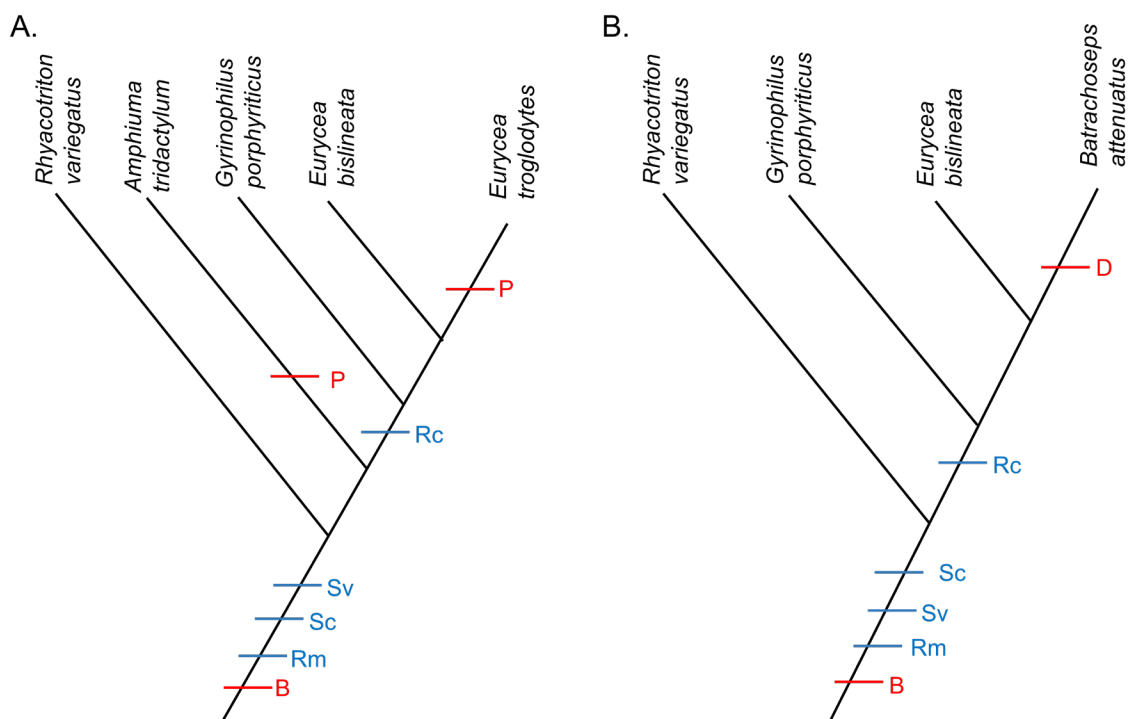


**Figure 35.** Simplified phylogeny of plethodontid salamanders and their relatives showing life history strategies (red) and cell types present in the VNO (blue). Phylogenies depict presence/absence in the VNO, not origin of cell types; it is assumed all cell types are ancestrally available. **A)** Results for larval stages of biphasic (B) species and for paedomorphic (P) species. **B)** Results for adult stages of biphasic (B) species and direct developing (D) species (Eisthen, 2000; Pyron & Wiens, 2011; Shen et al., 2016).

The relationship between cell type, phylogeny, and life history in the MOC will hopefully become clearer with further research, as the variety of cell types present across species and life stages does not obviously correlate strictly with life history. Life history appears to have some influence; for example the ultrastructure of the MOC of *B. attenuatus*, the most terrestrial species I examined, most closely resembles terrestrial anurans (Benzekri & Reiss, 2012) rather than its close relatives within the Plethodontidae. However, when examining species with aquatic life stages the interpretation of variation in cell types becomes more difficult.

The ultrastructure in the VNO across all species and stages indicates a stronger correlation between phylogeny and cell type than between life history and cell type. As previously stated, the VNO of all other amphibians contains microvillar receptor cells and ciliated supporting cells (Benzekri & Reiss, 2012; Eisthen, 2000; Hansen et al., 1998; Stuelpnagel & Reiss, 2005). In plethodontids, all four cell types are present in all species I examined. Paedomorphic species such as *E. troglodytes* more closely resemble other plethodontids that possess either direct development or metamorphic life histories, than paedomorphic species in other families such as Sirenidae or Amphiumidae (Eisthen, 2000).

Currently, the function of these four cell types in plethodontid salamanders is unclear. One role of supporting cells is to influence the olfactory signal transduction in receptor neurons (Lucero, 2013). However, the function of the distinct receptor cell types is less clear. Weiss et al. (2021) suggest two distinct transduction cascades. One contains ciliated receptor cells that relay signals from volatile chemicals, and the other utilizes microvillar receptor cells for the detection of nonvolatile chemicals. However, this research has been done in other taxa (see Benzekri & Reiss, 2012; Hansen, 2007; Nowack et al., 2013) and little is known about the specific correlation between function and cell type in plethodontids.

I began this study with three hypotheses:

1. Patterns of olfactory organization are consistent across species with the same life history strategy, regardless of evolutionary history.

2. Patterns of olfactory organization in paedomorphic species are consistent with the larvae of closely related species.
3. Aquatic olfactory features are lost or reduced in terrestrial, direct-developing species.

Hypothesis 1, as we have seen, was not supported by the data; there was much variation across species that could not be explained by life history, especially in the MOC, while phylogeny rather than life history appeared more important in the VNO. Hypothesis 2 was supported, in that *E. troglodytes* adults closely resembled “*E. bislineata*” larvae. Lastly, hypothesis 3 was difficult to evaluate, because some aquatic larval features of other salamanders, such as the presence of grooves lined by olfactory epithelium in the MOC, were not found in plethodontids or *Rhyacotriton*. However, it was certainly true that all of the larval and paedomorphic olfactory organs resembled each other in overall structure and differed from that of terrestrial adults of biphasic or direct-developing species.

This is the most extensive investigation of olfactory morphology and ultrastructure in a closely related group of amphibians attempted to date, however, I was only able to sample a few of the hundreds of species of plethodontids. More broad-scale morphological studies will help us more fully understand the relationship between morphology, phylogeny, and life history. More research utilizing electron microscopy is especially needed to understand the influence of phylogeny and life history on cell type. More research at the level of ultrastructure to not only identify morphological receptor cell types within the MOC and VNO, but also to relate them to specific odorant receptors

and ligands, is necessary to better understand the function of these cells. Further research to better document the correlation between phylogeny, life history, and morphology should be conducted on the other subfamily of Plethodontidae, Plethodontinae, or families outside of Caudata that also include a variety of life history strategies, such as Microhylidae (Anura) or Indotyphlidae (Gymnophiona) (Liedtke et al., 2022).

## REFERENCES

- AmphibiaWeb. (2022a). *Eurycea bislineata*. University of California, Berkeley, CA, USA. Accessed on 24 February 2022. <https://amphibiaweb.org/species/4049>
- AmphibiaWeb. (2022b). *Gyrinophilus porphyriticus*. University of California, Berkeley, CA, USA. Accessed on 24 February 2022. [https://amphibiaweb.org/cgi/amphib\\_query?where-genus=Gyrinophilus&where-species=porphyriticus](https://amphibiaweb.org/cgi/amphib_query?where-genus=Gyrinophilus&where-species=porphyriticus)
- AmphibiaWeb. (2022c). *Rhyacotriton variegatus*. University of California, Berkeley, CA, USA. Accessed on 24 February 2022. [https://amphibiaweb.org/cgi/amphib\\_query?where-genus=Rhyacotriton&where-species=variegatus&account=amphibiaweb](https://amphibiaweb.org/cgi/amphib_query?where-genus=Rhyacotriton&where-species=variegatus&account=amphibiaweb)
- Arnold, S. J., Kiemnec-Tyburczy, K. M., & Houck, L. D. (2017). The evolution of courtship behavior in plethodontid salamanders, contrasting patterns of stasis and diversification. *Herpetologica*, 73(3), 190.
- Baxi, K. N., Dorries, K. M., & Eisthen, H. L. (2006). Is the vomeronasal system really specialized for detecting pheromones? *Trends in Neurosciences*, 29(1), 1–7.
- Bazzola, J. J., & Russell, L. D. (1992). *Electron microscopy: Principles and techniques for biologists* (2nd ed.). Jones Bartlett Pub.
- Beachy, C. K., Ryan, T. J., & Bonett, R. M. (2017). How metamorphosis is different in plethodontids: Larval life history perspectives on life-cycle evolution. *Herpetologica*, 73(3), 252–258.

- Benzekri, N. A., & Reiss, J. O. (2012). Olfactory metamorphosis in the coastal tailed frog *Ascaphus truei* (Amphibia, Anura, Leiopelmatidae). *Journal of Morphology*, 273(1), 68–87.
- Bonett, R. M., Steffen, M. A., Lambert, S. M., Wiens, J. J., & Chippindale, P. T. (2014). Evolution of paedomorphosis in plethodontid salamanders: Ecological correlates and re-evolution of metamorphosis. *Evolution*, 68(2), 466–482.
- Brown, C. W. (1968). Additional observations on the function of the nasolabial grooves of plethodontid salamanders. *Copeia*, 1968(4), 728.
- Bruce, R. C. (1978). Life-history patterns of the salamander *Gyrinophilus porphyriticus* in the Cowee Mountains, North Carolina. *Herpetologica*, 34(1), 53–64.
- Dawley, E. M. (2017). Comparative morphology of plethodontid olfactory and vomeronasal organs: How snouts are packed. *Herpetological Monographs*, 31(1), 169–209.
- Dawley, E. M., & Bass, A. H. (1988). Organization of the vomeronasal organ in a plethodontid salamander. *Journal of Morphology*, 198(2), 243–255.
- Dawley, E. M., & Bass, A. H. (1989). Chemical access to the vomeronasal organs of a plethodontid salamander. *Journal of Morphology*, 200(2), 163–174.
- Duellman, W. E., & Trueb, L. (1986). *Biology of Amphibians*. McGraw - Hill Book Company.
- Doten, K., Bury, G. W., Rudenko, M., & Arnold, S. J. (2017). Courtship in the torrent salamander, *Rhyacotriton*, has an ancient and stable history. *Herpetological Conservation and Biology*, 12(2), 457–469.

- Eisthen, H. L. (2000). Presence of the vomeronasal system in aquatic salamanders. *Philosophical Transactions of the Royal Society of London. Series B: Biological Sciences*, 355(1401), 1209–1213.
- Eisthen, H. L., Dale, R. Sengelaub, Schroeder, D., M., & Alberts, J., R. (1994). Anatomy and forebrain projections of the olfactory and vomeronasal organs in axolotls (*Ambystoma mexicanum*). *Brain, Behavior and Evolution*, 44(2), 108–124.
- Gillette, J. R. (2002). Odor discrimination in the California slender salamander, *Batrachoseps attenuatus*: Evidence for self-recognition. *Herpetologica*, 58(2), 165–170.
- Hansen, A. (2007). Olfactory and solitary chemosensory cells: Two different chemosensory systems in the nasal cavity of the American alligator, *Alligator mississippiensis*. *BMC Neuroscience*, 8(1), 64.
- Hansen, A., Reiss, J. O., Gentry, C. L., & Burd, G. D. (1998). Ultrastructure of the olfactory organ in the clawed frog, *Xenopus laevis*, during larval development and metamorphosis. *The Journal of Comparative Neurology*, 398(2), 273–288.  
[https://doi.org/10.1002/\(SICI\)1096-9861\(19980824\)398:2<273::AID-CNE8>3.0.CO;2-Y](https://doi.org/10.1002/(SICI)1096-9861(19980824)398:2<273::AID-CNE8>3.0.CO;2-Y)
- Humason, G., L. (1979). *Animal Tissue Techniques* (4th ed.). W.H. Freeman and Company.
- Jurgens, J. D. (1971). The morphology of the nasal region of Amphibia and its bearing on the phylogeny of the group. *Ann Univ Stellenbosch*, 46A(2), 1–146.

- Kozak, K. H., Blaine, R. A., & Larson, A. (2005). Gene lineages and eastern North American palaeodrainage basins: Phylogeography and speciation in salamanders of the *Eurycea bislineata* species complex. *Molecular Ecology*, *15*(1), 191–207.
- Liedtke, H. C., Wiens, J. J., & Gomez-Mestre, I. (2022). The evolution of reproductive modes and life cycles in amphibians. *Nature Communications*, *13*(1), 7039. <https://doi.org/10.1038/s41467-022-34474-4>
- Lucero, M. (2013). Peripheral modulation of smell: fact or fiction? *Seminars in Cell & Developmental Biology*, *24*, 58–70.
- Nowack, C., Jordan, S., & Wittmer, C. (2013). The recessus olfactorius: A cryptic olfactory organ of anuran amphibians. In: *Chemical Signals in Vertebrates 12*. (pp. 37–40). Springer.
- Parsons, T. S. (1967). Evolution of the nasal structure in the lower tetrapods. *American Zoologist*, *7*(3), 397–413.
- Placyk, J. S., & Graves, B. M. (2002). Prey detection by vomeronasal chemoreception in a plethodontid salamander. *Journal of Chemical Ecology*, *28*(5), 1017–1036.
- Pyron, A. R., & Wiens, J. J. (2011). A large-scale phylogeny of amphibia including over 2800 species, and a revised classification of extant frogs, salamanders, and caecilians. *Molecular Phylogenetics and Evolution*, *61*(2), 543–583.
- Reiss, J. O., & Eisthen, H. L. (2008). Comparative anatomy and physiology of chemical senses in amphibians. In *Sensory Evolution on the Threshold: Adaptations in Secondarily Aquatic Vertebrates* (pp. 43–63). University of California Press.

- Schindelin, J., Arganda-Carreras, I., Frise, E., Kaynig, V., Longair, M., Pietzsch, T., Preibisch, S., Rueden, C., Saalfeld, S., Schmid, B., Tinevez, J.-Y., White, D. J., Hartenstein, V., Eliceiri, K., Tomancak, P., & Cardona, A. (2012). Fiji: An open-source platform for biological-image analysis. *Nature Methods*, *9*(7), 676–682.  
<https://doi.org/doi:10.1038/nmeth.2019>
- Shen, X.-X., Liang, D., Chen, M.-Y., Mao, R.-L., Wake, D. B., & Zhang, P. (2016). Enlarged multilocus data set provides surprisingly younger time of origin for the Plethodontidae, the largest family of salamanders. *Systematic Biology*, *65*(1), 66–81.
- Silva, L., & Antunes, A. (2017). Vomeronasal receptors in vertebrates and the evolution of pheromone detection. *Annual Review of Animal Biosciences*, *5*(1), 353–370.  
<https://doi.org/10.1146/annurev-animal-022516-022801>
- Stuelpnagel, J. T., & Reiss, J. O. (2005). Olfactory metamorphosis in the coastal giant salamander (*Dicamptodon tenebrosus*). *Journal of Morphology*, *266*(1), 22–45.
- Wake, D. (1966). Comparative osteology and evolution of the lungless salamanders, family Plethodontidae. *Memoirs of the Southern California Academy of Sciences*, *4*, 1-111.
- Weiss, L., Manzini, I., & Hassenklöver, T. (2021). Olfaction across the water–air interface in anuran amphibians. *Cell and Tissue Research*, *383*(1), 301–325.  
<https://doi.org/10.1007/s00441-020-03377-5>
- Wilder, I. W. (1925). The morphology of amphibian metamorphosis. Smith College.

## APPENDICES

## Appendix A: Specimen Data

**Table A1.** Collection data including species, date collected, location collected, and method used.

Specimen #	Species ID	Date collected	Locality	County	State	GPS Coordinates	SVL (mm)	TL (mm)	Sex	Method
JOR-21-001	<i>Batrachoseps attenuatus</i>	27 May 2021	4899 S Quarry Rd, Bayside	Humboldt	CA	40.826148, -124.038852	52	131	F	MicroCT
JOR-21-002	<i>Batrachoseps attenuatus</i>	27 May 2021	4900 S Quarry Rd, Bayside	Humboldt	CA	40.826148, -124.038852	52	68	M	MicroCT
JOR-21-010	<i>Gyrinophilus porphyriticus</i>	18 June 2021	St. Mary's River	Augusta	VA	37.931700, -79.157500	49	81	M	Histology
JOR-21-011	<i>Gyrinophilus porphyriticus</i>	18 June 2021	St. Mary's River	Augusta	VA	37.931700, -79.157500	49	86	M	Histology
JOR-21-014	<i>Eurycea bislineata</i>	18 June 2021	St. Mary's River	Augusta	VA	37.931700, -79.157500	41	92	F	TEM
JOR-21-015	<i>Eurycea bislineata</i>	18 June 2021	St. Mary's River	Augusta	VA	37.931700, -79.157500	18	31	F	Histology
JOR-21-016	<i>Eurycea bislineata</i>	18 June 2021	St. Mary's River	Augusta	VA	37.931700, -79.157500	22	41	M	Histology
JOR-21-019	<i>Eurycea bislineata</i>	19 June 2021	Mine's Run	Rockingham	VA	38.454400, -79.167400	41	96	M	TEM
JOR-21-020	<i>Eurycea bislineata</i>	19 June 2021	Mine's Run	Rockingham	VA	38.454400, -79.167400	24	43	F	Histology
JOR-21-021	<i>Eurycea bislineata</i>	19 June 2021	Mine's Run	Rockingham	VA	38.454400, -79.167400			ND	Histology
JOR-21-022	<i>Eurycea bislineata</i>	19 June 2021	Mine's Run	Rockingham	VA	38.454400, -79.167400	21	37	M	Histology
JOR-21-023	<i>Eurycea bislineata</i>	19 June 2021	Mine's Run	Rockingham	VA	38.454400, -79.167400	23	44	F	Histology
JOR-21-024	<i>Eurycea bislineata</i>	19 June 2021	Mine's Run	Rockingham	VA	38.454400, -79.167400	18	32	ND	Histology
JOR-21-025	<i>Eurycea bislineata</i>	19 June 2021	Mine's Run	Rockingham	VA	38.454400, -79.167400	24	46	ND	Histology
JOR-21-026	<i>Eurycea bislineata</i>	19 June 2021	Mine's Run	Rockingham	VA	38.454400, -79.167400	21	42	ND	Histology
JOR-21-027	<i>Eurycea bislineata</i>	19 June 2021	Mine's Run	Rockingham	VA	38.454400, -79.167400	19	35	F	Histology
JOR-21-028	<i>Eurycea bislineata</i>	19 June 2021	Mine's Run	Rockingham	VA	38.454400, -79.167400	41	93	ND	TEM
JOR-21-032	<i>Eurycea bislineata</i>	18 June 2021	Hone Quarry	Rockingham	VA	38.462262, -79.135493	21	40	M	Histology
JOR-21-033	<i>Eurycea bislineata</i>	18 June 2021	Hone Quarry	Rockingham	VA	38.462262, -79.135493	26	46	F	Histology
JOR-21-034	<i>Eurycea bislineata</i>	18 June 2021	Hone Quarry	Rockingham	VA	38.462262, -79.135493	23	38	M	Histology

Specimen #	Species ID	Date collected	Locality	County	State	GPS Coordinates	SVL (mm)	TL (mm)	Sex	Method
JOR-21-057	<i>Batrachoseps attenuatus</i>	1 October 2021	Arcata Community Forest	Humboldt	CA	40.875498, -124.072813	38	84	F	Histology
JOR-21-059	<i>Batrachoseps attenuatus</i>	1 October 2021	4899 S Quarry Rd, Bayside	Humboldt	CA	40.826148, -124.038852	58	148	M	Histology
JOR-21-065	<i>Batrachoseps attenuatus</i>	24 February 2022	Arcata Community Forest	Humboldt	CA	40.875498, -124.072813	43	100	M	TEM
JOR-21-066	<i>Batrachoseps attenuatus</i>	24 February 2022	Arcata Community Forest	Humboldt	CA	40.875498, -124.072813	41	79	F	TEM
JOR-21-074	<i>Gyrinophilus porphyriticus</i>	18 June 2021	St. Mary's River	Augusta	VA	37.931700, -79.157500			Larva	Histology
JOR-21-075	<i>Gyrinophilus porphyriticus</i>	18 June 2021	St. Mary's River	Augusta	VA	37.931700, -79.157500			Larva	Histology
JOR-21-076	<i>Eurycea bislineata</i>	18 June 2021	St. Mary's River	Augusta	VA	37.931700, -79.157500	20	39	Larva	Histology
JOR-21-077	<i>Eurycea bislineata</i>	18 June 2021	St. Mary's River	Augusta	VA	37.931700, -79.157500	24	48	M	Histology
JOR-21-078	<i>Gyrinophilus porphyriticus</i>	18 June 2021	St. Mary's River	Augusta	VA	37.931700, -79.157500			Larva	TEM
JOR-21-079	<i>Eurycea bislineata</i>	18 June 2021	St. Mary's River	Augusta	VA	37.931700, -79.157500			Larva	TEM
JOR-21-080	<i>Eurycea bislineata</i>	19 June 2021	Mine's Run	Rockingham	VA	38.454400, -79.167400			Larva	Histology
JOR-21-081	<i>Eurycea bislineata</i>	19 June 2021	Mine's Run	Rockingham	VA	38.454400, -79.167400			Larva	Histology
JOR-21-082	<i>Eurycea bislineata</i>	19 June 2021	Mine's Run	Rockingham	VA	38.454400, -79.167400			Larva	TEM
JOR-21-083	<i>Eurycea bislineata</i>	19 June 2021	Mine's Run	Rockingham	VA	38.454400, -79.167400			Larva	TEM
JOR-21-084	<i>Gyrinophilus porphyriticus</i>	18 June 2021	Hone Quarry	Rockingham	VA	38.462262, -79.135493	51	83	Larva	Histology
JOR-21-085	<i>Eurycea bislineata</i>	18 June 2021	Hone Quarry	Rockingham	VA	38.462262, -79.135493	19	32	Larva	Histology
JOR-21-086	<i>Eurycea bislineata</i>	18 June 2021	Hone Quarry	Rockingham	VA	38.462262, -79.135493			ND	TEM
JOR-21-087	<i>Eurycea bislineata</i>	18 June 2021	Hone Quarry	Rockingham	VA	38.462262, -79.135493			Larva	TEM
JOR-21-088	<i>Eurycea bislineata</i>	18 June 2021	Hone Quarry	Rockingham	VA	38.462262, -79.135493			Larva	TEM
JOR-21-091	<i>Batrachoseps attenuatus</i>	23 May 2022	4899 S Quarry Rd, Bayside	Humboldt	CA		51	121	F	Histology
JOR-21-092	<i>Batrachoseps attenuatus</i>	23 May 2022	4900 S Quarry Rd, Bayside	Humboldt	CA		52	134	F	Histology
JOR-21-093	<i>Gyrinophilus porphyriticus</i>	23 May 2022	Park Gap, Nantahala Mountains-Blue Ridge		NC	35.2183, -83.60076	84	136	M	TEM

Specimen #	Species ID	Date collected	Locality	County	State	GPS Coordinates	SVL (mm)	TL (mm)	Sex	Method
JOR-21-094	<i>Eurycea wilderae</i>	25 May 2022	Ball Creek Road near Coweeta Lab	35.05990, -83.4305	NC	35.05990, -83.4305	21	33	Larva	TEM
JOR-21-095	<i>Eurycea wilderae</i>	25 May 2022	Ball Creek Road near Coweeta Lab	35.05990, -83.4306	NC	35.05990, -83.4306	39	76	M	TEM
JOR-21-096	<i>Eurycea wilderae</i>	25 May 2022	Ball Creek Road near Coweeta Lab	35.05990, -83.4307	NC	35.05990, -83.4307	37	58	F	TEM
JOR-21-097	<i>Eurycea wilderae</i>	25 May 2022	Ball Creek Road near Coweeta Lab	35.05990, -83.4308	NC	35.05990, -83.4308	40	89	F	TEM
JOR-21-109	<i>Gyrinophilus porphyriticus</i>	26 May 2022	Whiteside Mountain, Highlands plateau	35.08073, -83.14378	NC	35.08073, -83.14378	67	110	M	TEM
JOR-21-110	<i>Eurycea wilderae</i>	28 May 2022	Highlands Biological Station		NC	35.0539, -83.189	34	78	M	TEM
JOR-21-120	<i>Eurycea wilderae</i>	2 June 2022	Blue Valley		NC		15	37	ND	Histology
JOR-21-121	<i>Eurycea wilderae</i>	2 June 2022	Blue Valley		NC		23	31	ND	Histology
JOR-21-132	<i>Gyrinophilus porphyriticus</i>	May 30 2022	Mount Mitchell, Bottom Brior Campground	35.76570, -82.2652	NC	35.76570, -82.2652	84	126	M	TEM
JOR-21-133	<i>Eurycea wilderae</i>	3 June 2022	Coker Lab, HBS		NC	35.0539, -83.189	34	68	F	TEM
JOR-21-133a	<i>Eurycea wilderae</i>	4 June	Long Branch Trail, near Standing Indian Campground		NC	35.07047, -83.4983	44	76	M	TEM
JOR-21-134	<i>Eurycea wilderae</i>	2 June 2022	East Fork Creek, Blue Valley		NC	35.11240, -82.747	22	40	Larva	TEM
JOR-21-155	<i>Eurycea wilderae</i>	5 June 2022	East Fork Creek, Blue Valley		NC	35.11240, -82.748	17	32	Larva	MicroCT
JOR-21-156	<i>Eurycea wilderae</i>	5 June 2022	East Fork Creek, Blue Valley		NC	35.11240, -82.749	10	16	Larva	TEM
JOR-21-157	<i>Eurycea wilderae</i>	5 June 2022	East Fork Creek, Blue Valley		NC	35.11240, -82.750	21	37	Larva	TEM
JOR-21-158	<i>Eurycea wilderae</i>	5 June 2022	East Fork Creek, Blue Valley		NC	35.11240, -82.751	19	37	Larva	TEM

Specimen #	Species ID	Date collected	Locality	County	State	GPS Coordinates	SVL (mm)	TL (mm)	Sex	Method
JOR-21-159	<i>Eurycea wilderae</i>	5 June 2022	East Fork Creek, Blue Valley		NC	35.11240, -82.752	9	15	Larva	TEM
JOR-21-160	<i>Gyrinophilus porphyriticus</i>	5 June 2022	Whiteside Mountain, Highlands plateau		NC	35.08073, -83.14377	15	17	Larva	TEM
JOR-21-161	<i>Gyrinophilus porphyriticus</i>	5 June 2022	Whiteside Mountain, Highlands plateau		NC	35.08073, -83.14378	57	92	M	TEM
JOR-21-162	<i>Eurycea wilderae</i>	7 June 2022	Deep Gap		NC	36.23930, -81.5153	38	99	M	MicroCT
JOR-21-163	<i>Eurycea wilderae</i>	7 June 2022	Whiteside Mountain, Highlands plateau		NC	35.08073, -83.14377	39	95	M	Histology
JOR-21-164	<i>Gyrinophilus porphyriticus</i>	7 June 2022	whiteside Mountain, Highlands plateau		NC	35.08073, -83.14378	67	105	M	MicroCT
JOR-21-165	<i>Gyrinophilus porphyriticus</i>	7 June 2022	whiteside Mountain, Highlands plateau		NC	35.08073, -83.14379	75	125	F	TEM
JOR-21-166	<i>Gyrinophilus porphyriticus</i>	7 June 2022	whiteside Mountain, Highlands plateau		NC	35.08073, -83.14380	68	116	M	TEM
JOR-21-167	<i>Gyrinophilus porphyriticus</i>	7 June 2022	whiteside Mountain, Highlands plateau		NC	35.08073, -83.14381	85	135	M	TEM
JOR-21-168	<i>Gyrinophilus porphyriticus</i>	7 June 2022	whiteside Mountain, Highlands plateau		NC	35.08073, -83.14382	24	47	Larva	TEM
JOR-21-179	<i>Eurycea sp.</i>	7 June 2022	Whiteside Mountain, Highlands Plateau		NC	35.08073, -83.14383	25	47	Larva	TEM
JOR-21-180	<i>Eurycea sp.</i>	6 June 2022	HBS Falls Creek		NC	35.0539, -83.189	30	61	Larva	TEM
JOR-21-181	<i>Eurycea sp.</i>	6 June 2022	HBS Falls Creek		NC	35.0539, -83.190	26	50	Larva	TEM
JOR-21-183	<i>Eurycea sp.</i>	6 June 2022	HBS Falls Creek		NC	35.0539, -83.191	24	45	ND	TEM
JOR-21-184	<i>Eurycea sp.</i>	6 June 2022	HBS Falls Creek		NC	35.0539, -83.192	22	46	ND	TEM
JOR-21-197	<i>Batrachoseps attenuatus</i>	22 June 2022	Arcata Community Forest	Humboldt	CA	40.87490, -124.0504	40	96	ND	TEM
JOR21-198	<i>Batrachoseps attenuatus</i>	18 July 2022	S. Quarry Rd., Bayside	Humboldt	CA	40.82200, -124.03501	49	118	F	TEM

Specimen #	Species ID	Date collected	Locality	County	State	GPS Coordinates	SVL (mm)	TL (mm)	Sex	Method
JOR-21-200	<i>Batrachoseps attenuatus</i>	10 August 2022	Arcata Community Forest	Humboldt	CA	40.87490827143456, -124.05048254857155	36	79	F	TEM
JOR-21-201	<i>Batrachoseps attenuatus</i>	15 August 2022	S. Quarry Rd., Bayside	Humboldt	CA	40.82200, -124.03501	41	101	F	TEM
JOR-21-202	<i>Batrachoseps attenuatus</i>	15 August 2022	S. Quarry Rd., Bayside	Humboldt	CA	40.82200, -124.03502	43	105	F	TEM
JOR-21-203	<i>Batrachoseps attenuatus</i>	1 September 2022	Arcata Community Forest	Humboldt	CA	40.8749, -124.0504	32	54	ND	TEM
JOR-21-204	<i>Batrachoseps attenuatus</i>	10 September 2022	Arcata Community Forest	Humboldt	CA	40.8749, -124.0505	41	94	M	TEM
JOR-21-205	<i>Batrachoseps attenuatus</i>	26 September 2022	Arcata Community Forest	Humboldt	CA	40.8749, -124.0506	40	82	F	TEM
JOR-21-206	<i>Batrachoseps attenuatus</i>	6 December 2022	Arcata Community Forest	Humboldt	CA	40.8749, -124.0507	43	94	M	TEM
JOR-21-207	<i>Batrachoseps attenuatus</i>	21 December 2022	Arcata Community Forest	Humboldt	CA	40.8749, -124.0508	36	64	ND	TEM
JOR-21-208	<i>Batrachoseps attenuatus</i>	21 December 2022	Arcata Community Forest	Humboldt	CA	40.8749, -124.0509	45	94	F	TEM
JOR-21-209	<i>Rhyacotriton variegatus</i>	6 March 2023	Arcata Community Forest	Humboldt	CA	40.8749, -124.0510	29	42	Larva	MicroCT
JOR-21-210	<i>Rhyacotriton variegatus</i>	6 March 2023	Arcata Community Forest	Humboldt	CA	40.8749, -124.0511	23	38	Larva	TEM
JOR-21-211	<i>Rhyacotriton variegatus</i>	6 March 2023	Arcata Community Forest	Humboldt	CA	40.8749, -124.0512	29	46	Larva	TEM
JOR-21-212	<i>Rhyacotriton variegatus</i>	6 March 2023	Arcata Community Forest	Humboldt	CA	40.8749, -124.0513	39	60	Larva	TEM
JOR-21-213	<i>Rhyacotriton variegatus</i>	24 March 2023	Arcata Community Forest	Humboldt	CA	40.8749, -124.0514	36	68	F	Histology
JOR-21-214	<i>Rhyacotriton variegatus</i>	24 March 2023	Arcata Community Forest	Humboldt	CA	40.8749, -124.0515	31	52	Larva	Histology
JOR-21-215	<i>Rhyacotriton variegatus</i>	24 March 2023	Arcata Community Forest	Humboldt	CA	40.8749, -124.0516	30	47	Larva	Histology
JOR-21-216	<i>Rhyacotriton variegatus</i>	24 March 2023	Arcata Community Forest	Humboldt	CA	40.8749, -124.0517	34	57	Larva	Histology
JOR-21-224	<i>Eurycea troglodytes</i>		Lost Maples	Bandera	TX	29.80728, -99.56970	34	55	M	MicroCT
JOR-21-227	<i>Rhyacotriton variegatus</i>	12 June 2023	Arcata Community Forest	Humboldt	CA	40.8749, -124.0522	29	47	Larva	TEM

Specimen #	Species ID	Date collected	Locality	County	State	GPS Coordinates	SVL (mm)	TL (mm)	Sex	Method
JOR-21-228	<i>Rhyacotriton variegatus</i>	12 June 2023	Arcata Community Forest	Humboldt	CA	40.8749, -124.0522	23	39	Larva	TEM
JOR-21-229	<i>Rhyacotriton variegatus</i>	12 June 2023	Arcata Community Forest	Humboldt	CA	40.8749, -124.0522	36	58	Larva	TEM
JOR-21-230	<i>Rhyacotriton variegatus</i>	12 June 2023	Arcata Community Forest	Humboldt	CA	40.8749, -124.0522	29	47	Larva	TEM
JOR-21-231	<i>Rhyacotriton variegatus</i>	12 June 2023	Arcata Community Forest	Humboldt	CA	40.8749, -124.0522	34	58	Larva	TEM
JOR-21-232	<i>Eurycea troglodytes</i>	Spring 2023	Lost Maples	Bandera	TX	29.80728, -99.56970	27	46	M	TEM
JOR-21-233	<i>Eurycea troglodytes</i>	Spring 2024	Lost Maples	Bandera	TX	29.80728, -99.56970	27	42	F	TEM
JOR-21-234	<i>Eurycea troglodytes</i>	Spring 2025	Lost Maples	Bandera	TX	29.80728, -99.56970	29	46	F	TEM
JOR-21-235	<i>Eurycea troglodytes</i>	Spring 2026	Lost Maples	Bandera	TX	29.80728, -99.56970	27	45	F	TEM
JOR-21-236	<i>Eurycea troglodytes</i>	Spring 2027	Lost Maples	Bandera	TX	29.80728, -99.56970	27	44	F	TEM
JOR-21-237	<i>Eurycea troglodytes</i>	10 Feb 2023	Johnson Ranch	Kerr	TX	30.04616, -99.678375	28	40	M	Histology
JOR-21-238	<i>Eurycea troglodytes</i>	10 Feb 2023	Johnson Ranch	Kerr	TX	30.04616, -99.678375	31	50	M	Histology
JOR-21-239	<i>Eurycea troglodytes</i>	10 Feb 2023	Johnson Ranch	Kerr	TX	30.04616, -99.678375	27	39	F	Histology
JOR-21-240	<i>Eurycea troglodytes</i>	10 Feb 2023	Johnson Ranch	Kerr	TX	30.04616, -99.678375	32	43	F	Histology
JOR-21-241	<i>Eurycea troglodytes</i>	10 Feb 2023	Johnson Ranch	Kerr	TX	30.04616, -99.678375	32	45	F	Histology
JOR-21-242	<i>Rhyacotriton variegatus</i>	5 July 2023	Arcata Community Forest	Humboldt	CA	40.8749, -124.050	46	73	F	TEM
JOR-21-274	<i>Batrachoseps attenuatus</i>	17 September 2023	Arcata Community Forest	Humboldt	CA	40.8749, -124.050	36	82	F	TEM
JOR-21-275	<i>Rhyacotriton variegatus</i>	30 September 2023	Arcata Community Forest	Humboldt	CA	40.8749, -124.050	50	78	F	TEM
JOR-21-276	<i>Rhyacotriton variegatus</i>	30 September 2023	Arcata Community Forest	Humboldt	CA	40.8749, -124.050	50	79	M	TEM
JOR-21-277	<i>Rhyacotriton variegatus</i>	30 September 2023	Arcata Community Forest	Humboldt	CA	40.8749, -124.050	50	80	M	TEM
JOR-21-278	<i>Rhyacotriton variegatus</i>	30 September 2023	Arcata Community Forest	Humboldt	CA	40.8749, -124.050	36	55	M	TEM
JOR-21-279	<i>Rhyacotriton variegatus</i>	30 September 2023	Arcata Community Forest	Humboldt	CA	40.8749, -124.050	53	85	M	TEM

Specimen #	Species ID	Date collected	Locality	County	State	GPS Coordinates	SVL (mm)	TL (mm)	Sex	Method
JOR-21-280	<i>Rhyacotriton variegatus</i>	30 September 2023	Arcata Community Forest	Humboldt	CA	40.8749, -124.050	40	60	M	TEM
JOR-21-281	<i>Gyrinophilus porphyriticus</i>	Fall 2023	Jacoby Falls Trail	Lycoming	PA	41.3773, -76.9185	110	70	Larvae	MicroCT
JOR-21-283	<i>Gyrinophilus porphyriticus</i>	Fall 2023	Jacoby Falls Trail	Lycoming	PA	41.3773, -76.9185	70	115	Larvae	TEM
JOR-21-284	<i>Gyrinophilus porphyriticus</i>	Fall 2023	Jacoby Falls Trail	Lycoming	PA	41.3773, -76.9185	56	77	Larvae	TEM
JOR-21-285	<i>Gyrinophilus porphyriticus</i>	Fall 2023	Jacoby Falls Trail	Lycoming	PA	41.3773, -76.9185	57	90	Larvae	TEM
JOR-21-286	<i>Gyrinophilus porphyriticus</i>	Fall 2023	Jacoby Falls Trail	Lycoming	PA	41.3773, -76.9185	55	84	Larvae	TEM

## Appendix B: MicroCT Data

**Table A2.** Methods used for MicroCT scanning including species, target type, voxel size, voltage, and current.

Specimen #	Species	Target	Voxel size (mm)	Voltage (kV)	Current ( $\mu$ A)
JOR-21-002	<i>Batrachoseps attenuatus</i>	Tungsten	0.008041	85	104
JOR-21-155	<i>Eurycea wilderae</i> larva	Tungsten	0.00456517	89	74
JOR-21-162	<i>Eurycea wilderae</i> adult	Tungsten	0.0087639	125	69
JOR-21-164	<i>Gyrinophilus porphyriticus</i> adult	Tungsten	0.00985747	75	101
JOR-21-209	<i>Rhyacotriton variegatus</i> larva	Tungsten	0.00875338	52	119
JOR-21-213	<i>Rhyacotriton variegatus</i> adult	Tungsten	0.00925454	73	110
JOR-21-224	<i>Eurycea troglodytes</i>	Tungsten	0.00843655	60	120
JOR-21-281	<i>Gyrinophilus porphyriticus</i> larva	Tungsten	0.00644108	50	56